Ministry for Primary Industries
Manatū Ahu Matua

The 2012 stock assessment of paua (*Haliotis iris*) for PAU 5D

New Zealand Fisheries Assessment Report 2013/57

D. Fu

ISSN 1179-5352 (online)
ISBN 978-0-478-42075-3 (online)

October 2013

New Zealand Government

Growing and Protecting New Zealand

Requests for further copies should be directed to:

Publications Logistics Officer
Ministry for Primary Industries
PO Box 2526
WELLINGTON 6140

Email: brand@mpi.govt.nz
Telephone: 0800 00 83 33
Facsimile: 04-894 0300

This publication is also available on the Ministry for Primary Industries websites at:
http://www.mpi.govt.nz/news-resources/publications.aspx
http://fs.fish.govt.nz go to Document library/Research reports

EXECUTIVE SUMMARY

Fu, D. (2013). The 2012 stock assessment of paua (*Haliotis iris*) for PAU 5D

***New Zealand Fisheries Assessment Report 2013/57*. 51 p.**

This report summarises the stock assessment for PAU 5D which includes fishery data up to the 2011–12 fishing year. The report describes the model structure and output, including current and projected stock status. The stock assessment is implemented as a length-based Bayesian estimation model, with point estimates of parameters based on the mode of the joint posterior distribution, and uncertainty of model estimates investigated using the marginal posterior distributions generated from Markov chain-Monte Carlo simulation.

The data fitted in the assessment model were: (1) a standardised CPUE series based on the early CELR data, (2) a standardised CPUE series based on recent PCELR data, (3) commercial catch sampling length frequency series (CSLF), (4) tag-recapture length increment data, and (5) maturity-at-length data. The research diver survey data was not included in the assessment because there is concern that the data is not a reliable index of abundance and the data is not representative of the whole PAU 5D stock.

The base case model (5.2) estimated that the spawning stock population in 2012 (B_{2012}) was about 35% (28–44%) of B_0 . The model projection made for three years assuming current catch levels and using recruitments re-sampled from the recent model estimates, suggested that the spawning stock abundance will increase to about 39% (27–54%) of B_0 over the next three years. The projection also indicated that the probability of the spawning stock biomass being above the target (40% B_0) will increase from about 15% in 2012 to 43% in 2015, and that the stock status is very unlikely to be below the soft (20% B_0) and hard limits (10% B_0).

Most data sets used in the model were from a limited number of locations, and were most likely not representative of the whole QMA. Three sensitivity trials were considered to be equally as plausible as the base case model: run 5.5 where the early CPUE series was removed, run 6.3 where the growth was fixed high, and run 6.5 where the growth was fixed low. Runs 5.5, 6.3, and 6.5 estimated $B_{current}$ to be about 24%, 22%, and 60% of B_0 respectively. All runs indicated that it was very unlikely the stock will fall below the soft or hard limits and suggested that biomass would increase over the next three years at current levels of catch, but the four runs differed in their assessment of the status of the stock relative to the target.

1. INTRODUCTION

1.1 Overview

This report summarises the stock assessment for PAU 5D (from the Waitaki River mouth to Colac Bay on the southern coast of the South Island, (Figure 1 & 2) with the inclusion of data to the end of 2011–12 fishing year. The report describes the model structure and output, including current and projected stock status. The stock assessment is conducted with the length-based Bayesian estimation model first used in 1999 for PAU 5B (Breen et al. 2000a) with revisions made for subsequent assessments in PAU 5B (Breen et al. 2000b, Breen & Smith 2008), PAU 4 (Breen & Kim 2004a), PAU 5A (Breen & Kim 2004b, Breen & Kim 2007, Fu & Mackenzie 2010a, b), PAU 7 (Andrew et al. 2000, Breen et al. 2001, Breen & Kim 2003, 2005, McKenzie & Smith 2009, Fu 2012). PAU 5D was last assessed in 2006 (Breen & Kim 2007) and before that in 2000 (Breen et al. 2000a). The model was published by Breen et al. (2003).

The five sets of data used in the assessment model were: (1) a standardised CPUE series covering 1990–2001 based on CELR data (CPUE), (2) a standardised CPUE series covering 2002–2012 based on PCELR data (PCPUE), (3) A commercial catch sampling length frequency series (CSLF), (4) tag-recapture length increment data, and (5) maturity-at-length data. The research diver survey covered only the Catlin areas, therefore the RDSI and RDLF data were not included in the model. Catch history was an input to the model, encompassing commercial, recreational, customary, and illegal catch. Another document describes the datasets that are used in the stock assessment and the updates that were made for the previous assessment (Fu et al. 2013).

The assessment was made in several steps. First, the model was fitted to the data with arbitrary weights on the various datasets. The weights were then iteratively adjusted to produce balanced residuals among the datasets where the standard deviation of the normalised residuals was close to one for each dataset. The length frequency data were further down-weighted using the method by Francis (2011). The fit obtained is the mode of the joint posterior distribution of parameters (MPD). Next, from the resulting fit, Markov chain-Monte Carlo (MCMC) simulations were made to obtain a large set of samples from the joint posterior distribution. From this set of samples, forward projections were made with a set of agreed indicators obtained. Sensitivity trials were explored by comparing MPD fits made with alternative model assumptions.

This document describes the model structure and assumptions, the fits to the data, estimates of parameters and indicators, and projection results. This report fulfils Objective 1 "Undertake a stock assessment for PAU 5D, using a length-based Bayesian model" of the Ministry of Fisheries (now the Ministry for Primary Industries) project PAU200802.

1.2 Description of the fishery

The paua fishery was summarised by Schiel (1992), and in numerous previous assessment documents (e.g., Schiel 1989, McShane et al. 1994, 1996, Breen et al. 2000a, 2000b, 2001, Breen & Kim 2003, 2004a, 2004b, 2007). A further summary is not presented here.

2. MODEL

This section gives an overview of the model used for stock assessment of PAU 5D in 2012; for full description see Breen et al. (2003). The model was developed for use in PAU 5B in 1999 and has been revised each year for subsequent assessments, in many cases echoing changes made to the rock

lobster assessment model (Kim et al. 2004), which is a similar but more complex length-based Bayesian model. The last revision made to the model was the 2011 assessment model of PAU 7 (Fu 2012), with the main change being that a penalty function was imposed to encourage the mean of recruitment deviation to be close to one.

2.1 Model description

The model partitioned the paua stock into a single sex population, with length classes from 70 mm to 170 mm, in groups of 2 mm (i.e., from 70 to under 72 mm, 72 mm to under 74 mm, etc.). The largest length bin is well above the maximum size observed. The stock was assumed to reside in a single, homogeneous area. The partition accounted for numbers of paua by length class within an annual cycle, where movement between length classes was determined by the growth parameters. Paua entered the partition following recruitment and were removed by natural mortality and fishing mortality.

The model annual cycle was based on the fishing year. Note that model references to "year" within this paper refer to the fishing year, and are labelled as the most recent calendar year, i.e., the fishing year 1998–99 is referred to as "1999" throughout. References to calendar years are denoted specifically.

The models were run for the years 1965–2012. Catches were collated for 1974–2012, and were assumed to increase linearly between 1965 and 1973 from 0 to the 1974 catch level. Catches included commercial, recreational, customary, and illegal catch, and all catches occurred at the same time step.

Recruitment was assumed to take place at the beginning of the annual cycle, and length at recruitment was defined by a uniform distribution with a range between 70 and 80 mm. Recruitment deviations were assumed known and equal to 1 for the years up to 1980. This was ten years before length data were available (loosely based on the approximate time taken for recruited paua to appear at the right hand end of the length distribution). The stock-recruitment relationship is unknown for paua, but is likely to be weak (Shepherd et al. 2001). A relationship may exist on small scales, but may not be apparent when large-scale data are modelled (Breen et al. 2003). No explicit stock-recruitment relationship has been modelled in previous assessments. The Shellfish Working Group suggested assuming a Beverton-Holt stock-recruitment relationship with a steepness of 0.75 for the base case.

Maturity does not feature in the population partition. The model estimated proportions mature with the inclusion of length-at-maturity data. Growth and natural mortalities were also estimated within the model.

The models used two selectivities: the commercial fishing selectivity and research diver survey selectivity — both assumed to follow a logistic curve (see later). The commercial fishing selectivity was shifted to the right by 5 mm for 2006–2015 (assuming that the increase of minimum harvest size extends to the projection period).

The model is implemented in AD Model Builder™ (Otter Research Ltd., http://otter-rsch.com/admodel.htm) version 9.0.65, compiled with the MinGW 4.50 compiler.

2.1.1 Estimated parameters

Parameters estimated by the model are as follows. The parameter vector is referred to collectively as θ.

$\ln(R0)$	natural logarithm of base recruitment
M	instantaneous rate of natural mortality
g_1	expected annual growth increment at length L_1
g_2	expected annual growth increment at length L_2
ϕ	CV of the expected growth increment
α	parameter that defines the variance as a function of growth increment
β	parameter that defines the variance as a function of growth increment
$\Delta_{\max}$	maximum growth increment
l_{50}^{g}	length at which the annual increment is half the maximum
l_{95}^{g}	length at which the annual increment is 95% of the maximum
l_{95-50}^{g}	difference between l_{50}^{g} and l_{95}^{g}
q^{I}	scalar between recruited biomass and CPUE
q^{I_2}	scalar between recruited biomass and PCPUE
q^{J}	scalar between numbers and the RDSI
L_{50}	length at which maturity is 50%
L_{95-50}	interval between L_{50} and L_{95}
T_{50}	length at which research diver selectivity is 50%
T_{95-50}	difference between T_{50} and T_{95}
D_{50}	length at which commercial diver selectivity is 50%
D_{95-50}	difference between D_{50} and D_{95}
$\tilde{\sigma}$	common component of error
h	shape of CPUE *vs.* biomass relation
ε	vector of annual recruitment deviations, estimated from 1977 to 2004
H	steepness of the Beverton-Holt stock-recruitment relationship

2.1.2 Constants

l_k	length of a paua at the midpoint of the k^{th} length class (l_k for class 1 is 71 mm, for class 2 is 73 mm and so on)
σ_{MIN}	minimum standard deviation of the expected growth increment (assumed to be 1 mm)
σ_{obs}	standard deviation of the observation error around the growth increment (assumed to be 0.25 mm)
MLS_t	minimum legal size in year t (assumed to be 125 mm for all years)
$P_{k,t}$	a switch based on whether abalone in the k^{th} length class in year t are above the minimum legal size (MLS) ($P_{k,t}$ = 1) or below ($P_{k,t}$ = 0)
a, b	constants for the length-weight relation, taken from Schiel & Breen (1991) (2.592E-08 and 3.322 respectively, giving weight in kg)
w_k	the weight of an abalone at length l_k
ϖ^{I}	relative weight assigned to the CPUE dataset. This and the following relative weights were varied between runs to find a basecase with balanced residuals.
ϖ^{I2}	relative weight assigned to the PCPUE dataset

ϖ^J	relative weight assigned to the RDSI dataset
ϖ^r	relative weight assigned to RDLF dataset
ϖ^s	relative weight assigned to CSLF dataset
ϖ^{mat}	relative weight assigned to maturity-at-length data
ϖ^{tag}	relative weight assigned to tag-recapture data
κ_t^s	normalised square root of the number of paua measured greater than 113 mm in CSLF records for each year, normalised by the lowest year
κ_t^r	normalised square root of the number of paua measured greater than 89 mm in RDLF records for each year, normalised by the lowest year
$U^{\max}$	exploitation rate above which a limiting function was invoked (0.65 for the base case)
μ_M	mean of the prior distribution for *M*, based on a literature review by Shepherd & Breen (1992)
σ_M	assumed standard deviation of the prior distribution for *M*
σ_ε	assumed standard deviation of recruitment deviations in log space (part of the prior for recruitment deviations)
n_ε	number of recruitment deviations
L_1	length associated with g_1 (75 mm)
L_2	length associated with g_2 (120 mm)

2.1.3 Observations

C_t	observed catch in year *t*
I_t	standardised CPUE in year *t*
$I2_t$	standardised PCPUE in year *t*
σ_t^I	standard deviation of the estimate of observed CPUE in year *t*, obtained from the standardisation model
σ_t^{I2}	standard deviation of the estimate of observed PCPUE in year *t*, obtained from the standardisation model
J_t	standardised RDSI in year *t*
σ_t^J	the standard deviation of the estimate of RDSI in year t, obtained from the standardisation model
$p_{k,t}^r$	observed proportion in the k^{th} length class in year *t* in RDLF
$p_{k,t}^s$	observed proportion in the k^{th} length class in year *t* in CSLF
l_j	initial length for the j^{th} tag-recapture record
d_j	observed length increment of the *j*th tag-recapture record
Δt_j	time at liberty for the j^{th} tag-recapture record
p_k^{mat}	observed proportion mature in the k^{th} length class in the maturity dataset

2.1.4 Derived variables

$R0$	base number of annual recruits
$N_{k,t}$	number of paua in the k^{th} length class at the start of year t
$N_{k,t+0.5}$	number of paua in the k^{th} length class in the mid-season of year t
$R_{k,t}$	recruits to the model in the k^{th} length class in year t
g_k	expected annual growth increment for paua in the k^{th} length class
σ^{g_k}	standard deviation of the expected growth increment for paua in the k^{th} length class, used in calculating $\mathbf{G}$
$\mathbf{G}$	growth transition matrix
B_t	spawning stock biomass at the beginning of year t
$B_{t+0.5}$	spawning stock biomass in the mid-season of year t
B_0	equilibrium spawning stock biomass assuming no fishing and average recruitment from the period in which recruitment deviations were estimated.
B_{init}	spawning stock biomass at the end of initialisation phase (or B_{1964})
B_t^r	biomass of paua above the MLS at the beginning of year t
$B_{t+0.5}^r$	biomass of paua above the MLS in the mid-season of year t
B_0^r	equilibrium biomass of paua above the MLS assuming no fishing and average recruitment from the period in which recruitment deviations were estimated
B_{init}^r	biomass of paua above the MLS at the end of initialisation phase (or B_{1964}^r)
U_t	exploitation rate in year t
A_t	the complement of exploitation rate
$SF_{k,t}$	finite rate of survival from fishing for paua in the kth length class in year t
V_k^r	relative selectivity of research divers for paua in the kth length class
V_k^s	relative selectivity of commercial divers for paua in the kth length class
$\sigma_{k,t}^r$	error of the predicted proportion in the k^{th} length class in year t in RDLF data
n_t^r	relative weight (effective sample size) of the RDLF data in year t
$\sigma_{k,t}^s$	error of the predicted proportion in the k^{th} length class in year t in CSLF data
n_t^s	relative weight (effective sample size)of the CSLF data in year t
σ_j^d	standard deviation of the predicted length increment for the j^{th} tag-recapture record
σ_j^{tag}	total error predicted for the j^{th} tag-recapture record
σ_k^{mat}	error of the proportion mature-at-length for the k^{th} length class
$-\ln(\mathbf{L})$	negative log-likelihood
f	total function value

2.1.5 Predictions

$\hat{I}_t$	predicted CPUE in year *t*
$\hat{I}2_t$	predicted PCPUE in year *t*
$\hat{J}_t$	predicted RDSI in year *t*
$\hat{p}^r_{k,t}$	predicted proportion in the k^{th} length class in year *t* in research diver surveys
$\hat{p}^s_{k,t}$	predicted proportion in the k^{th} length class in year *t* in commercial catch sampling
$\hat{d}_j$	predicted length increment of the j^{th} tag-recapture record
$\hat{p}^{mat}_k$	predicted proportion mature in the k^{th} length class

2.1.6 Initial conditions

The initial population is assumed to be in equilibrium with zero fishing mortality and the base recruitment. The model is run for 60 years with no fishing to obtain near-equilibrium in numbers-at-length. Recruitment is evenly divided among the first five length bins:

(1) $R_{k,t} = 0.2R0$ for $1 \le k \le 5$

(2) $R_{k,t} = 0$ for $k > 5$

A growth transition matrix is calculated inside the model from the estimated growth parameters. If the growth model is linear, the expected annual growth increment for the *k*th length class is:

(3) $$\Delta l_k = \left(\frac{L_2 g_1 - L_1 g_2}{g_1 - g_2} - l_k \right) \left[1 - \left(1 + \frac{g_1 - g_2}{L_1 - L_2} \right) \right]$$

The model uses the AD Model Builder™ function *posfun*, with a dummy penalty, to ensure a positive expected increment at all lengths, using a smooth differentiable function. The *posfun* function is also used with a real penalty to force the quantity $\left(1 + \frac{g_1 - g_2}{L_1 - L_2} \right)$ to remain positive. If the growth model is exponential (used for the base case), the expected annual growth increment for the *k*th length class is:

(4) $$\Delta l_k = g_1 \left(g_2 / g_1 \right)^{(l_k - L_1)/(L_2 - L_1)}$$

again using posfun with a dummy penalty to ensure a positive expected increment at all lengths. If the inverse logistic growth model is used), the expected annual growth increment for the *k*th length class is:

(5) $$\Delta l_k = \frac{\Delta_{\max}}{\left(1 + \exp\left(\ln(19) \left(\left(l_k - l^g_{50} \right) / \left(l^g_{95} - l^g_{50} \right) \right) \right) \right)}$$

The standard deviation of g_k is assumed to be proportional to g_k with minimum σ_{MIN}:

$$\sigma^{g_k} = \left(g_k\phi - \sigma_{MIN}\right)\left(\frac{1}{\pi}\tan^{-1}\left(10^6\left(g_k\phi - \sigma_{MIN}\right)\right) + 0.5\right) + \sigma_{MIN} \quad (6)$$

Or a more complex functional form between the growth increment and its standard deviation can be defined as:

$$\sigma^{g_k} = \left(\alpha\left(g_k\right)^{\beta} - \sigma_{MIN}\right)\left(\frac{1}{\pi}\tan^{-1}\left(10^6\left(\alpha\left(g_k\right)^{\beta} - \sigma_{MIN}\right)\right) + 0.5\right) + \sigma_{MIN} \quad (7)$$

From the expected increment and standard deviation for each length class, the probability distribution of growth increments for a paua of length l_k is calculated from the normal distribution and translated into the vector of probabilities of transition from the k^{th} length bin to other length bins to form the growth transition matrix **G**. Zero and negative growth increments are permitted, i.e., the probability of staying in the same bin or moving to a smaller bin can be non-zero.

In the initialisation, the vector $\mathbf{N_t}$ of numbers-at-length is determined from numbers in the previous year, survival from natural mortality, the growth transition matrix **G,** and the vector of recruitment $\mathbf{R_t}$:

$$\mathbf{N_t} = \left(\mathbf{N_{t\text{-}1}}\, e^{-M}\right) \bullet \mathbf{G} + \mathbf{R_t} \quad (8)$$

where the dot (•) denotes matrix multiplication.

2.1.7 Dynamics

2.1.7.1 Sequence of operations

After initialising, the first model year is 1965 and the model is run through to 2012. In the first nine years the model is run with an assumed catch vector, because it is unrealistic to assume that the fishery was in a virgin state when the first catch data became available in 1974. The assumed catch vector rises linearly from zero to the 1974 catch. These years can be thought of as an additional part of the initialisation, but they use the dynamics described in this section.

Model dynamics are sequenced as follows.

- Numbers at the beginning of year *t*-1 are subjected to fishing, then natural mortality, then growth to produce the numbers at the beginning of year *t*.
- Recruitment is added to the numbers at the beginning of year *t*.
- Biomass available to the fishery is calculated and, with catch, is used to calculate the exploitation rate, which is constrained if necessary.
- Half the exploitation rate (but no natural mortality) is applied to obtain mid-season numbers, from which the predicted abundance indices and proportions-at-length are calculated. Mid-season numbers are not used further.

2.1.7.2 Main dynamics

For each year *t*, the model calculates the start-of-the-year biomass available to the commercial fishery. Biomass available to the commercial fishery is:

$$B_t = \sum_k N_{k,t} V_k^s w_k \quad (9)$$

$$V_k^{t,s} = \frac{1}{1+19^{-\left((l_k - D_{50})/D_{95-50}\right)}} \quad \text{for } t < 2006 \quad (10)$$

$$V_k^{t,s} = \frac{1}{1+19^{-\left((l_k - D_{50} - 5)/D_{95-50}\right)}} \quad \text{for } t \geq 2006 \quad (11)$$

The observed catch is then used to calculate the exploitation rate, constrained for all values above U^{max} with the *posfun* function of AD Model Builder™. If the ratio of catch to available biomass exceeds U^{max}, then exploitation rate is constrained and a penalty is added to the total negative log-likelihood function. Let minimum survival rate A_{min} be 1-U^{max} and survival rate A_t be 1-U_t:

$$A_t = 1 - \frac{C_t}{B_t} \quad \text{for } \frac{C_t}{B_t} \leq U^{\max} \quad (12)$$

$$A_t = 0.5 A_{\min}\left[1 + \left(3 - \frac{2\left(1 - \frac{C_t}{B_t}\right)}{A_{\min}}\right)^{-1}\right] \quad \text{for } \frac{C_t}{B_t} > U^{\max} \quad (13)$$

The penalty invoked when the exploitation rate exceeds U^{max} is:

$$1000000\left(A_{\min} - \left(1 - \frac{C_t}{B_t}\right)\right)^2 \quad (14)$$

This prevents the model from exploring parameter combinations that give unrealistically high exploitation rates. Survival from fishing is calculated as:

$$SF_{k,t} = 1 - (1 - A_t) P_{k,t} \quad (15)$$

or

$$SF_{k,t} = 1 - (1 - A_t) V_k^s \quad (16)$$

The vector of numbers-at-length in year *t* is calculated from numbers in the previous year:

$$\mathbf{N_t} = \left(\left(\mathbf{SF_{t-1}} \otimes \mathbf{N_{t-1}}\right) \mathrm{e}^{-M}\right) \bullet \mathbf{G} + \mathbf{R_t} \quad (17)$$

where $\otimes$ denotes the element-by-element vector product. The vector of recruitment, $\mathbf{R_t}$, is determined from *R0*, estimated recruitment deviations, and the stock-recruitment relationship:

(18) $$R_{k,t} = 0.2R0e^{\left(\varepsilon_t - 0.5\sigma_t^2\right)} \frac{B_{t-1+0.5}}{B_0} \Big/ \left(1 - \frac{5H-1}{4H}\left(1 - \frac{B_{t-1+0.5}}{B_0}\right)\right) \qquad \text{for } 1 \le k \le 5$$

(19) $$R_{k,t} = 0 \qquad \text{for } k > 5$$

The recruitment deviation parameters ε_t were estimated for all years from 1980. The recruitment deviations were constrained to have a mean of 1 in arithmetic space.

The model predicts CPUE in year *t* from mid-season recruited biomass, the scaling coefficient, and the shape parameter:

(20) $$\hat{I}_t = q^I \left(B_{t+0.5}\right)^h$$

Available biomass $B_{t+0.5}$ is the mid-season vulnerable biomass after half the catch has been removed (no natural mortality is applied, because the time over which half the catch is removed might be short). It is calculated as in equation (9), but using the mid-year numbers, $N_{k,t+0.5}$:

(21) $$N^{vuln}_{k,t+0.5} = N_{k,t}\left(1 - \frac{\left(1-A_t\right)}{2} V^s_k\right).$$

Similarly,

(22) $$\hat{I}2_t = q^{I2}\left(B_{t+0.5}\right)^h = Xq^I\left(B_{t+0.5}\right)^h$$

The same shape parameter *h* is used for both series: experimentation outside the model showed that this was appropriate despite the different units of measurement for the two series. The predicted research diver survey index is calculated from mid-season model numbers in bins greater than 89 mm length, taking into account research diver selectivity-at-length:

(23) $$N^{res}_{k,t+0.5} = N_{k,t}\left(1 - \frac{\left(1-A_t\right)}{2} V^r_k\right)$$

(24) $$\hat{J}_t = q^J \sum_{k=11}^{55} N^{res}_{k,t+0.5}$$

where the scalar is estimated and the research diver selectivity V^r_k is calculated from:

(25) $$V^r_k = \frac{1}{1+19^{-\left(\left(l_k - T_{50}\right)/T_{95-50}\right)}}$$

The model predicts proportions-at-length for the RDLF from numbers in each length class for lengths greater than 89 mm:

$$(26) \qquad \hat{p}^{r}_{k,t} = \frac{N^{res}_{k,t+0.5}}{\sum_{k=11}^{51} N^{res}_{k,t+0.5}} \qquad \text{for } 11 \le k < 51$$

Predicted proportions-at-length for CSLF are similar:

$$(27) \qquad \hat{p}^{s}_{k,t} = \frac{N^{vuln}_{k,t+0.5}}{\sum_{k=23}^{51} N^{vuln}_{k,t+0.5}} \qquad \text{for } 23 \le k < 51$$

The predicted increment for the *j*th tag-recapture record, using the linear model, is:

$$(28) \qquad \hat{d}_j = \left(\frac{\beta g_\alpha - \alpha g_\beta}{g_\alpha - g_\beta} - L_j \right) \left[1 - \left(1 + \frac{g_\alpha - g_\beta}{\alpha - \beta} \right)^{\Delta t_j} \right]$$

where Δt_j is in years. For the exponential model (used in the base case) the expected increment is

$$(29) \qquad \hat{d}_j = \Delta t_j g_\alpha \left(g_\beta / g_\alpha \right)^{(L_j - \alpha)/(\beta - \alpha)}$$

The error around an expected increment is:

$$(30) \qquad \sigma_j^{\,d} = \left(\hat{d}_j \phi - \sigma_{MIN} \right) \left(\frac{1}{\pi} \tan^{-1} \left(10^6 \left(\hat{d}_j \phi - \sigma_{MIN} \right) \right) + 0.5 \right) + \sigma_{MIN}$$

Predicted maturity-at-length is:

$$(31) \qquad \hat{p}^{mat}_k = \frac{1}{1 + 19^{-\left((l_k - L_{50}) / L_{95-50} \right)}}$$

2.1.8 Fitting

2.1.8.1 Likelihoods

The distribution of CPUE is assumed to be normal-log and the negative log-likelihood is:

$$(32) \qquad -\ln(\mathbf{L}) \left(\hat{I}_t \mid \theta \right) = \frac{\left(\ln(I_t) - \ln\left(\hat{I}_t \right) \right)^2}{2 \left(\sigma_t^I \tilde{\sigma} / \varpi^I \right)^2} + \ln\left(\sigma_t^I \tilde{\sigma} / \varpi^I \right) + 0.5 \ln(2\pi)$$

and similarly for PCPUE:

(33) $$-\ln(\mathbf{L})\left(\hat{I}2_t \mid \theta\right) = \frac{\left(\ln\left(I2_t\right) - \ln\left(\hat{I}2_t\right)\right)^2}{2\left(\sigma_t^{I2}\tilde{\sigma}\,/\,\varpi^{I2}\right)^2} + \ln\left(\sigma_t^{I2}\tilde{\sigma}\,/\,\varpi^{I2}\right) + 0.5\ln\left(2\pi\right)$$

The distribution of the RDSI is also assumed to be normal-log and the negative log-likelihood is:

(34) $$-\ln(\mathbf{L})\left(\hat{J}_t \mid \theta\right) = \frac{\left(\ln\left(J_t\right) - \ln\left(\hat{J}_t\right)\right)^2}{2\left(\sigma_t^{J}\tilde{\sigma}\,/\,\varpi^{J}\right)^2} + \ln\left(\sigma_t^{J}\tilde{\sigma}\,/\,\varpi^{J}\right) + 0.5\ln\left(2\pi\right)$$

The proportions-at-length from CSLF data are assumed to follow a multinomial distribution, with a standard deviation that depends on the effective sample size (see Section 2.2.9.3) and the weight assigned to the data:

(35) $$\sigma_{k,t}^{s} = \frac{\tilde{\sigma}}{\varpi^{s} n_t^{s}}$$

The negative log-likelihood is:

(36) $$-\ln(\mathrm{L})\left(\hat{p}_{k,t}^{s} \mid \theta\right) = \frac{p_{s,t}^{s}}{\sigma_{k,t}^{s}}\left(\ln\left(p_{k,t}^{s} + 0.01\right) - \ln\left(\hat{p}_{k,t}^{s} + 0.01\right)\right)$$

The likelihood for research diver sampling is analogous. Errors in the tag-recapture dataset were also assumed to be normal. For the *j*th record, the total error is a function of the predicted standard deviation (equation (30)), observation error, and weight assigned to the data:

(37) $$\sigma_j^{tag} = \tilde{\sigma} / \varpi^{tag}\sqrt{{\sigma_{obs}}^2 + \left(\sigma_j^{d}\right)^2}$$

and the negative log-likelihood is:

(38) $$-\ln(\mathbf{L})\left(\hat{d}_j \mid \theta\right) = \frac{\left(d_j - \hat{d}_j\right)^2}{2\left(\sigma_j^{tag}\right)^2} + \ln\left(\sigma_j^{tag}\right) + 0.5\ln\left(2\pi\right)$$

The proportion mature-at-length was assumed to be normally distributed, with standard deviation analogous to proportions-at-length:

(39) $$\sigma_k^{mat} = \frac{\tilde{\sigma}}{\varpi^{mat}\sqrt{p_k^{mat} + 0.1}}$$

The negative log-likelihood is:

(40) $$-\ln(\mathbf{L})\left(\hat{p}_k^{mat} \mid \theta\right) = \frac{\left(p_k^{mat} - \hat{p}_k^{mat}\right)^2}{2\left(\sigma_k^{mat}\right)^2} + \ln\left(\sigma_k^{mat}\right) + 0.5\ln\left(2\pi\right)$$

2.1.8.2 Normalised residuals

These are calculated as the residual divided by the relevant σ term used in the likelihood. For CPUE, the normalised residual is

$$(41) \qquad \frac{\ln\left(I_t\right)-\ln\left(\hat{I}_t\right)}{\left(\sigma_t^I \tilde{\sigma} \Big/ \varpi^I\right)}$$

and similarly for PCPUE and RDSI. For the CSLF proportions-at-length, the residual is:

$$(42) \qquad \frac{p_{k,t}^s - \hat{p}_{k,t}^s}{\sigma_{k,t}^s}$$

and similarly for proportions-at-length from the RDLFs. Because the vectors of observed proportions contain many empty bins, the residuals for proportions-at-length include large numbers of small residuals, which distort the frequency distribution of residuals. When presenting normalised residuals from proportions-at-length, we arbitrarily ignore normalised residuals less than 0.05.

For tag-recapture data, the residual is:

$$(43) \qquad \frac{d_j - \hat{d}_j}{\sigma_j^{tag}}$$

and for the maturity-at-length data the residual is:

$$(44) \qquad \frac{p_k^{mat} - \hat{p}_k^{mat}}{\sigma_k^{mat}}$$

2.1.8.3 Dataset weights

The abundance data (CPUE and RDSI) were included in the model with log-normal likelihood. The observed standard deviation of each index (σ_t^I for CPUE) was modified by the weight assigned to the dataset (ϖ_I) and $\tilde{\sigma}$ to obtain the model weighted standard deviation (see equations 32–34). The weight of the dataset was determined iteratively so that the standardised deviation of the normalised residuals was close to one. The proportions at length (CSLF and RDLF) were included in the model with a multinomial likelihood. The length frequencies for individual years were assigned initial weights (effective sample size), based on a sample size that represented the best least squares fit of $\log(cv_i) \sim \log(P_i)$, where cv_i was the bootstrap CV for the ith proportion, P_i. (See Figure A1, Appendix A, for a plot of this relationship). The weights for individual years (n_t^s for CSLF) were then modified by the weight assigned to the dataset (ϖ_s for CSLF) and to obtain the model weights for the observations (See equation 35).

In previous assessments, the weight of each dataset was determined iteratively so that the standardised deviation of the normalised residuals was close to one. In this assessment, the same procedure was

used to determine the weight assigned to the CPUE data. The observed and final CV for the CPUE data used in the base case are summarised in Table 1 . For the CSLF data, we used an alternative weighting scheme following Francis (2011), where the weight was determined as

(45) $$\varpi^s = 1/\mathrm{var}_t\left[\left(\overline{O}_t^s - \overline{E}_t^s\right)/\left(v_t^s / n_t^s\right)^{0.5}\right]$$ (Method TA1.8, table A1 in Francis 2011)

Where

(46) $$\overline{O}_t^s = \sum_k p_{k,t}^s l_k$$

(47) $$\overline{E}_t^s = \sum_k \hat{p}_{k,t}^s l_k$$

(48) $$v_t^s = \sum_k \left(l_k\right)^2 \hat{p}_{k,t}^s - \left(\overline{E}_t^s\right)^2$$

The weight for the RDLF dataset was calculated similarly. This weighting method allows for the possibility of substantial correlations within a dataset, and generally produces relatively smaller sample size, thus down-weighting the composition data (Francis 2011). The actual and estimated sample sizes for the commercial catch and research diver proportions at length are given in Table 4.
.

2.1.8.4 Priors and bounds

Bayesian priors were established for all estimated parameters (Table 2). Most were incorporated simply as uniform distributions with upper and lower bounds set arbitrarily wide so as not to constrain the estimation. The prior probability density for *M* was a normal-log distribution with mean μ_M and standard deviation σ_M . The contribution to the objective function of estimated *M* = *x* is:

(49) $$-\ln(\mathbf{L})(x \mid \mu_M, \sigma_M) = \frac{\left(\ln\left(M\right) - \ln\left(\mu_M\right)\right)^2}{2{\sigma_M}^2} + \ln\left(\sigma_M\sqrt{2\pi}\right)$$

The prior probability density for the vector of estimated recruitment deviations ε , was assumed to be normal with a mean of zero and a standard deviation of 0.4. The contribution to the objective function for the whole vector is:

(50) $$-\ln\left(\mathbf{L}\right)(\varepsilon \mid \mu_\varepsilon, \sigma_\varepsilon) = \frac{\sum_{i=1}^{n_\varepsilon}\left(\varepsilon_i\right)^2}{2{\sigma_\varepsilon}^2} + \ln\left(\sigma_\varepsilon\right) + 0.5\ln\left(2\pi\right).$$

Constant parameters are given in Table 3

2.1.8.5 Penalty

A penalty is applied to exploitation rates higher than the assumed maximum (equation 12); it is added to the objective function after being multiplied by an arbitrary weight (1E6) determined by experiment.

AD Model Builder™ also has internal penalties that keep estimated parameters within their specified bounds, but these should have no effect on the final outcome, because choice of a base case excludes the situations where parameters are estimated at or near a bound.

2.1.9 Fishery indicators

The assessment calculates the following quantities from their posterior distributions: the model's mid-season spawning and recruited biomass for 2012 ($B_{current}$ and $B^r_{current}$) and for the projection period (B_{proj} and B^r_{proj}).

In the 2010 assessment for PAU 5A, Fu & McKenzie (2010a, 2010b) reported B_{init}; the spawning stock biomass at the end of the initialisation phase (the equilibrium biomass assuming that recruitment is equal to base recruitment and with no fishing), and B_0; the equilibrium spawning stock biomass assuming that recruitment is equal to the average recruitment from the period for which recruitment deviations were estimated (B_0 normally differs from B_{init}). In this assessment a constraint was placed on the recruitment deviations so that their average is 1 for the period in which they are estimated, based on the parameterisation of Bull et al (2012). This ensures that the average recruitment for the period in which they are estimated (1980–2008) is close to R_0, and as a result B_{init} will be close to B_0. This assessment also reports the following fishery indictors:

$\%B_0$	Ratio of current and projected spawning biomass to B_0
$\%B_{msy}$	Ratio of current and projected spawning biomass to B_{msy}
$\Pr(> B_{msy})$	Probability that current and projected spawning biomass greater than B_{msy}
$\Pr(> B_{current})$	Probability that projected spawning biomass greater than $B_{current}$
$\%B^r_0$	Ratio of current and projected recruited biomass to B^r_0
$\%B^r_{msy}$	Ratio of current and projected recruited biomass to B^r_{msy}
$\Pr(> B^r_{msy})$	Probability that current and projected recruit-sized biomass greater than B^r_{msy}
$\Pr(> B^r_{current})$	Probability that projected recruit-sized biomass greater than $B^r_{current}$
$\Pr(B_{proj} > 40\%B_0)$	Probability that projected spawning biomass is greater than 40% B_0
$\Pr(B_{proj} < 20\%B_{msy})$	Probability that projected spawning biomass less than 20% B_0
$\Pr(B_{proj} < 10\%B_{msy})$	Probability that projected spawning biomass less than 10% B_0
$\Pr(U_{proj} > U_{40\%B0})$	Probability that projected exploitation rate greater than $U_{40\%B0}$

2.1.10 Markov chain-Monte Carlo (MCMC) procedures

AD Model Builder™ uses the Metropolis-Hastings algorithm. The step size is based on the standard errors of the parameters and their covariance relationships, estimated from the Hessian matrix.

For the MCMCs in this assessment single long chains were run, starting at the MPD estimate. The base case was 5 million simulations long and samples were saved, regularly spaced by 5000. The value of $\tilde{\sigma}$ was fixed to that used in the MPD run because it may be inappropriate to let a variance component change during the MCMC.

2.1.11 Development of base case and sensitivity model runs

To develop the base case, a number of exploratory runs were carried out where the following aspects were investigated:

- Determining the weights of proportion-at-length datasets based on SDNRs or using the TA1.8 method (see Section 2.1.8.3).
- The use of an exponential versus a linear or an inverse-logistic growth model.
- The use of alternative maturity-at-length estimates.
- The effect of including RDSI and RDLF data.
- The change of commercial catch selectivity in and after 2006.

The sample sizes of the CSLF data determined using the TA1.8 method were much lower than those calculated using the SDNRs based method. There was little difference in the fits to the CSLF between the two methods. The SFWG decided to use the TA1.8 method in subsequent model runs, as this method accounted for the potential correlations in the proportion-at-length data.

Three alternative growth models were investigated. Although the linear and the inverse-logistic models have fitted the tag-recapture data better, with more balanced residuals throughout the length range, they have resulted in poor model fits to the CSLF data. Therefore the exponential growth model was used in the assessment models. For all the models, the estimated CV of the mean growth was very high (over 60%), which is likely to be due to the lack of data from the smaller size range. The SFWG decided to fix the CV of the mean growth to be 30%, based on the estimate of the growth using the tag-recapture data from PAU 5A, which had similar mean growth and variability as the data from PAU 5D.

The maturity data were collected from the Catlin area only. The data suggested that 50% maturity (L_{50}) was at about 80 mm, which is much less than that typically estimated for other paua stocks. An exploratory run was carried out using maturity data from PAU 5A, where L_{50} was estimated to be about 90 mm. However, this made negligible difference to the estimated spawning stock biomass.

The research diver surveys were conducted only in the Catlins area (east and west strata). The abundance indices and length frequencies derived from these surveys were unlikely to represent the trend for the whole PAU 5D stock. The SFWG decided not to include the RDSI and the RDLF in the assessment. An exploratory run fitting to the RDSI and RDLF suggested that the estimated stock status was insensitive to the inclusion of the RDSI and RDLF data.

The commercial catch length frequencies used in this assessment included only the years in which there were samples from each of the statistical areas within PAU 5D (i.e. 024, 025, 026 and 030). Therefore, scaled length frequencies from 1998, 2002–04, 2007, and 2009–2012 were used. There appeared to be much less paua under the minimum harvest size (MHS) in the catch samples over recent years, as there has been a voluntary increase in the MHS from 125 mm to 130 mm since 2006. Therefore it was decided to shift the commercial catch selectivity by 5 mm after 2006 for the assessment models.

The Shellfish WG suggested a base case (5.2) following discussions of exploratory model runs. The base case model excluded the RDSI and RDLF data, used the TA1.8 method to determine the weight of the CSLF data, and estimated *M* and the growth within the model (CV of the mean growth was fixed at 30%). Also, in the base case, the commercial catch selectivity was shifted by 5 mm in and after 2006, and the CPUE shape parameter was fixed at 1 assuming a linear relationship between CPUE and abundance.

A number of sensitivity runs were carried out: Run 5.3, 5.4, 5.5 and 5.6 dropped one dataset at a time (tag-recapture, CSLF, early and recent CPUE indices were removed from the model, respectively).

Runs 6.3 and 6.5 fixed the growth parameters at values representing either fast growth ($g_1 = 32.5$ and $g_2 = 10$) or slow growth ($g_1 = 24.5$ and $g_2 = 5$); model 7.2 assumed higher values of non-commercial catch; model 8.2 fixed natural mortality *M* at 0.1. Models 9.2 and 9.3 investigated different values of the CPUE shape parameter. A summary description of base case and sensitivity model runs is given in Table 5.

3. RESULTS

3.1 MPD base case

Model estimates of objective function values (negative log-likelihood), parameters, and indicators for the base case are given in the first column of Table 6. The base case fits the two observed CPUE abundance indices very well (Figure 3) and the model appears to have captured both the trend and inter-annual variations in the two sets of relative abundance indices. Fits to commercial proportions-at-length are very reasonable (Figures 4) although fits to the left-hand side of the distribution were less adequate for the most recent three years.

QQ plots of the residuals from the fits to the abundance indices show no apparent departure from the normality assumption (Figure 5). Francis (2011) suggested using the predicted annual mean length (across length classes) as a diagnostic tool for the proportion-at-length data, because there were potential correlations in residuals for individual length classes. Figure 6 shows a reasonable match between the predicted and observed mean length for the CSLF. The standard deviations of residuals for the annual mean length were close to unity for both proportion-at-length datasets (see Table 6).

The estimate of *M* was 0.15, close to the assumed mean of the prior distribution, 0.10. Estimates of growth parameters suggested a mean annual growth of 28.6 mm at 75 mm and 7.5 mm at 120 mm (see Table 6). The midpoint of the commercial fishery selectivity was 123 mm, slightly below the MLS, and this ogive was very narrow (see Table 6). Length at 50% and full maturity were estimated to be approximately 79 mm and 91 mm respectively (
Figure 7-left). The estimated growth transition matrix appeared to have accounted for most of the variability in the growth data (
Figure 7-right). Residuals in the fits to the tag-recapture data suggested that the model may have over-estimated the growth for the small and large size classes (Figure 8). However, it was noted that the sample size was small for these size ranges in the data.

The MPD estimates for the spawning stock biomass (mature animals) and recruited biomass (animals at or above the MLS) are shown in Figure 9. Both recruited and spawning biomass decreased substantially from 1965, but increased moderately since 2003 (when the voluntary quota shelving took place). The current spawning stock biomass ($B_{current}$) was estimated to be about 33% of B_0 and the current recruit-sized biomass ($B^r_{current}$) was about 24% of B^r_0 (see Table 6).

The profile likelihood on R_0 (as a proxy for B_0) indicated that the likelihood function values of the CPUE abundance indices were sensitive to the lower values of B_0, but was unable to differentiate higher values of B_0, whereas the commercial catch length frequencies appeared to be sensitive to a wider range of values of the initial biomass (Figure 10).

3.2 MPD sensitivity trials

Model estimates of objective function values (negative log-likelihood), parameters, and indicators for sensitivity trials are given in Table 6. A comparison of model estimates of spawning stock biomass between base case and sensitivity runs is shown in Figure 11. A comparison of model fits between base case and sensitivity runs is shown in Figures A2–A9, Appendix A.

The influence on model estimates from observational datasets was investigated by removing one dataset at a time. Removing the tag-recapture dataset (Run 5.3) resulted in different estimates of growth parameters, suggesting that growth estimates were predominately determined by the tag-recapture data although they were also influenced by the length frequency data fitted in the model. Removing the CSLF data (Run 5.5) increased estimates of biomass by more than 200% (Figure 11–first row). Removing the early CPUE series (Run 5.5), the model showed a much steeper decline in spawning stock biomass between 1990 and 2001 (see Figure 11); Removing the recent CPUE series (Run 5.6), the model show a much flatter trend in spawning stock biomass between 2002 and 2012 (see Figure 11). When either of the two CPUE series was dropped, the estimated current stock status was lower than that of the base case.

Run 6.3 fixed the growth parameters at values representing fast growth ($g_1 = 32.5$ and $g_2 = 10$), loosely based on the data from Catlins West (Figure A3). These assumed values implied a more productive stock, and the model estimated a higher *M*, and lower spawning stock biomass (Figure 11–second row). Run 6.5 fixed the growth parameters at values representing slow growth ($g_1 = 24.5$ and $g_2 = 5$), loosely based on data from Catlins west). These assumed values implied a less productive stock, and the model estimated a lower *M*, and much higher spawning stock biomass (see Figure 11–second row). With both models, the fits to the CPUE data are not significantly different to the base case (Figures A3), although the fits to the CSLF data were slightly worse for some of the recent years (Figure A4).

Model 7.2 used higher values of non-commercial catch where both recreational and illegal catch were assumed to increase from 2 t in 1974 to 30 t in 2012 (the base case assumed that both recreational and illegal catch increased linearly from 2 t in 1974 to 10 t in 2005, and has remained constant at 10 t between 2006 and 2012). As a result, the model estimated higher biomass trajectory (see Figure 11–third row), but the estimated current stock status was similar to the base case, with $B_{current}$ estimated to be about 36% B_0 (see Table 6). There was almost no difference in the fits to the CPUE and CSLF data compared to the base case (Figures A5 and A6).

When *M* was fixed at 0.1 (Run 8.2), the model fitted both the CPUE and CSLF data poorly (Figures A7 and A8). The overall objective function values was higher than that of the base case (see Table 6). The model also estimated a higher B_0 and a lower current stock status than the base case (see Figure 11–third row).

The base case fixed the CPUE shape parameter at 1, assuming a linear relationship between CPUE and abundance. Models 9.2 and 9.3 fixed the CPUE shape parameter value at 0.4 and 0.8 respectively (0.4 was close to the value of *h* if estimated freely within the model), assuming that the relationship between CPUE and abundance is hyper-stable. However, this has little effect on the fits to the CPUE data (Figure A9), nor on the estimates of the current stock status (see Figure 11–fourth row).

In general most estimated model parameters were not significantly different among sensitivity trials. Estimates of *M* ranged from 0.11 to 0.17. Estimates of $B_{current}$ ranged from 22% to 66% B_0 and appeared to be sensitive to the assumed value of growth and the exclusion of CSLF or the early CPUE series.

3.3 MCMC results

Because most data sets used in the assessment were from a limited number of locations, and were most likely not representative of the whole QMA, the SFWG suggested carrying out further MCMC runs for models 5.2 5.5, 6.3, and 6.5 to capture the uncertainty in the stock assessment. All four runs were considered to be equally plausible.

3.4 Marginal posterior distributions and the Bayesian fit

The main diagnostic used for the MCMC was the trace plots of the posterior samples. For the base case, the MCMC traces show good mixing (Figure 12), the posteriors for estimated parameters and indicators were generally well formed, and MPDs were mostly near the centres but tended to be below the median of the biomass posterior (Figure 13). In general, there is no evidence of non-convergence for estimated parameters and key biomass indicators for all models. The posteriors are summarised in Table 7 for the base case, Table 8 for run 5.5, Table 9 for run 6.3 and Table 10 for run 6.5.

For the base case, the posteriors of fits to CSLF were very reasonable (Figure 14-left). The posteriors of fits to the abundance indices appear adequate and the predictions encompass the range of the observed values in most years (Figure 14-right). The estimates of recruitment deviations suggested a period of relatively low recruitment in the late 1990s and relatively high recruitment in the early 2000s. The recruitment since 2004 appears to be close to the long term average (Figure 15-left). Estimated exploitation rates peaked in 2002, but have drastically decreased since then (Figure 15-left).

The posterior distribution of spawning stock biomass for all models is shown in Figure 16. These estimated biomass trajectories generally show a rapid decline since the inception of the fishery, followed by a gradual recovery after 2002.

The base case model (5.2) estimated that the unfished spawning stock biomass (B_0) was about 2285 t (2099–2487 t) and that the spawning stock population in 2012 ($B_{current}$) was about 35% (28–44%) of B_0 (Table 7). When the early CPUE series were dropped (Run 5.5), the model showed a much steeper decline in spawning stock biomass between 1990 and 2001, and estimated that $B_{current}$ was about 26% (20–35%) of B_0 (Table 8). When the growth parameters were fixed at higher values (Run 6.3), $B_{current}$ was estimated to be about 22% (19–27%) of B_0 (Table 9). When the growth parameters were fixed at lower values (Run 6.5), $B_{current}$ was estimated to be about 60% (50–72%) of B_0 (Table 10).

Deterministic B_{msy} was also calculated in the 2012 assessment using posterior distributions of estimated parameters, with the median of B_{msy} estimated at 624 t, 704 t, 556 t and 912 t for the 5.2, 5.5, 6.3 and 6.5 models respectively. The corresponding exploitation rates (U_{msy}) were estimated at 26%, 20%, 25% and 31% respectively. The assessment also calculated $U_{\%40B_0}$, which is the exploitation rate at which the spawning stock biomass will stabilise at 40% B_0. $U_{\%40B_0}$ was estimated at 16%, 13%, 16%, and 16% for the 5.2, 5.5, 6.3, and 6.5 models respectively.

Figure 17 shows the trajectories of exploitation rate as a ratio of $U_{\%40B_0}$ and spawning stock biomass as a ratio of B_0 from the start of assessment period 1965 to 2012 for each of the MCMC model runs.

Each point on the trajectory represents the estimated annual stock status: the value on the x axis is the mid-season spawning stock biomass (as a ratio of B_0) and the value on the y axis is the corresponding exploitation rate (as a ratio $U_{\%40B_0}$) for that year. For all the models, the trajectory started in 1965 when the SSB is close to B_0 and the exploitation rate is close to 0. Models 5.2, 5.5 and 6.3 indicated an early phase of the fishery where the exploitation rates were below $U_{\%40B_0}$ and the SSBs were above 40% B_0 and a later phase where the exploitation rates were above $U_{\%40B_0}$ and the SSBs were below 40%.

3.5 Projections

Model projections assuming current catch levels and using recruitments resampled from the recent model estimates were made for models 5.2, 5.5, 6.3, and 6.5. The projections made for base case and sensitivity trials all suggested that the biomass is likely to increase in the short term at the current catch level.

For the base case, the three-year projection suggested that the spawning stock abundance will increase to about 39% (27–54%) of B_0 over the next three years (Table 11). The projection also indicated that the probability of the spawning stock biomass being above the target (40% B_0) will increase from about 15% in 2012 to 43% in 2015, and that the stock status is very unlikely to be below the soft (20% B_0) or hard limit (10%) in the short term.

When the early CPUE series was dropped (Run 5.5), the model projections suggested an increase in biomass over the next 3 years, and a probability of being above the target of 40% B_0 by 2015 of 3%. The probability of the spawning stock being below 20% B_0 is about 4% (Table 12)

When the growth parameters were fixed at higher values (Run 6.3), the model projections also suggested an increase in biomass over the next 3 years, with the probability of being above the target of 2%, and a probability of the spawning stock being below 20% B_0 of about 10% (Table 13).

When the growth parameters were fixed at lower values (Run 6.5), the model projections suggested the stock biomass is currently above the target and will increase over the next 3 years (Table 14).

Projections from the different models estimated between 40 and 100% probabilities of the biomass in 2015 being above B_{msy}. These projections suggest that the stock is very unlikely (less than 10%) to fall below the soft or hard limits at the current level of catch.

4. DISCUSSION

This report assesses PAU 5D and includes fishery data up to the 2011–12 fishing year. The base model fitted the two CPUE series and the CSLF data, and estimated growth parameters within the model. Because most data sets used in the model were from a limited number of locations, and were most likely not representative of the whole QMA, MCMC runs were conducted for the base case and three additional sensitivity runs to address uncertainties in various aspects of the input data. All four runs were considered to be equally plausible and showed that it was very unlikely the stock will fall below the soft or hard limits, and suggested that biomass would increase over the next three years at

current levels of catch, but the four runs differed in their assessment of the status of the stock relative to the target.

The assessment used CPUE as an index of abundance. The assumption that CPUE indexes abundance is questionable. The literature on abalone suggests that CPUE is difficult to use in abalone stock assessments because of serial depletion. This can happen when fishers can deplete unfished or lightly fished beds and maintain their catch rates by moving to new areas, thus CPUE stays high while the biomass is actually decreasing. For PAU 5D, there is some additional uncertainty associated with the early CPUE: the standardisations suggested that there were different trends among statistical areas (the overall indices were unlikely to track abundance as the weights for each area cannot be easily determined); the level of decline in the CPUE indices appeared too small for the early stage of the fishery. The model results were sensitive to the inclusion/exclusion of the early CPUE indices.

Another source of uncertainty is the catch data. The commercial catch is unknown before 1974 and is estimated with uncertainly before 1995. Although we think the effect is minor, major differences may exist between the catches we assume and what was actually taken. In addition, non-commercial catch estimates are poorly determined and could be substantially different from what was assumed, although generally non-commercial catches appear to be relatively small compared with commercial catch. The estimate of illegal catch in particular is uncertain.

Tag-recapture data was mainly from the Catlin areas and therefore may not reflect fully the average growth in this population. Model estimates of stock status were sensitive to the range of possible growth values examined. Maturity data was collected from Catlin West and may not represent this population either. However, model estimates appeared not to be sensitive to the values of maturity-at-length. Length frequency data collected from the commercial catch may not represent the commercial catch with high precision. The research diver survey covered only the Catlin Area, the abundance indices and associated length frequencies were considered unlikely to represent the trend in the whole population.

The model treats the whole of the assessed area of PAU 5D as if it were a single stock with homogeneous biology, habitat and fishing pressures. The model assumes homogeneity in recruitment and natural mortality, and that growth has the same mean and variance. However it is known that paua in some areas have stunted growth, and others are fast-growing.

Heterogeneity in growth can be a problem for this kind of model (Punt 2003). Variation in growth is addressed to some extent by having a stochastic growth transition matrix based on increments observed in several different places; similarly the length frequency data are integrated across samples from many places.

The effect is likely to make model results optimistic. For instance, if some local stocks are fished very hard and others not fished, recruitment failure can result because of the depletion of spawners. Spawners must breed close to each other and the dispersal of larvae is unknown and may be limited. Recruitment failure is a common observation in overseas abalone fisheries, so local processes may decrease recruitment, an effect that the current model cannot account for.

Another source of uncertainty is that fishing may cause spatial contraction of populations (Shepherd & Partington 1995), or that some populations become relatively unproductive after initial fishing (Gorfine & Dixon 2000). If this happens, the model will overestimate productivity in the population as a whole. Past recruitments estimated by the model might instead have been the result of serial depletion.

5. ACKNOWLEDGMENTS

This work was supported by a contract from the Ministry of Fisheries (PAU200802 Objective 1). Thank you to Paul Breen for developing the stock assessment model that was used in this assessment and for the use of major proportions of the 2006 report for this update. Thank you to the Shellfish Working Group for all the advice provided throughout the assessment process. Thank you to Reyn Naylor for reviewing the manuscript.

6. REFERENCES

Andrew, N.L.; Breen, P.A.; Naylor, J.R.; Kendrick, T.H.; Gerring, P. (2000). Stock assessment of paua (*Haliotis iris*) in PAU 7 in 1998–99. *New Zealand Fisheries Assessment Report 2000/49*. 40 p.

Breen, P.A.; Andrew, N.L.; Kendrick, T.H. (2000a). Stock assessment of paua (*Haliotis iris*) in PAU 5B and PAU 5D using a new length-based model. *New Zealand Fisheries Assessment Report 2000/33*. 37 p.

Breen, P.A.; Andrew, N.L.; Kendrick, T.H. (2000b). The 2000 stock assessment of paua (*Haliotis iris*) in PAU 5B using an improved Bayesian length-based model. *New Zealand Fisheries Assessment Report 2000/48*. 36 p.

Breen, P.A.; Andrew, N.L.; Kim, S.W. (2001). The 2001 stock assessment of paua (*Haliotis iris*) in PAU 7. *New Zealand Fisheries Assessment Report 2001/55*. 53 p.

Breen, P.A.; Kim, S.W. (2003). The 2003 stock assessment of paua (*Haliotis iris*) in PAU 7. *New Zealand Fisheries Assessment Report 2003/35*. 112 p.

Breen, P.A.; Kim, S.W. (2004a). The 2004 stock assessment of paua (*Haliotis iris*) in PAU 4. *New Zealand Fisheries Assessment Report 2004/55*. 79 p.

Breen, P.A.; Kim, S.W. (2004b). The 2004 stock assessment of paua (*Haliotis iris*) in PAU 5A. *New Zealand Fisheries Assessment Report 2004/40*. 86 p.

Breen, P.A.; Kim, S.W. (2005). The 2005 stock assessment of paua (*Haliotis iris*) in PAU 7. *New Zealand Fisheries Assessment Report 2005/47*. 114 p.

Breen, P.A.; Kim, S.W. (2007). The 2006 stock assessment of paua (*Haliotis iris*) stocks PAU 5A (Fiordland) and PAU 5D (Otago). *New Zealand Fisheries Assessment Report 2007/09*. 164 p.

Breen, P.A.; Kim, S.W.; Andrew, N.L. (2003). A length-based Bayesian stock assessment model for abalone. *Marine and Freshwater Research 54(5):* 619–634.

Breen, P.A.; Smith, A.N.H. (2008). The 2007 assessment for paua *(Haliotis iris)* stock PAU 5B (Stewart Island).

Bull, B.; Francis, R.I.C.C.; Dunn, A.; McKenzie, A.; Gilbert, D.J.; Smith, M.H.; Bian, R. (2012). CASAL (C++ algorithmic stock assessment laboratory): CASAL User Manual v2.30-2012/03/21. *NIWA Technical Report* 135.

Francis, R.I.C.C. (2011). Data weighting in statistical fisheries stock assessment models. *Canadian Journal of Fisheries and Aquatic Sciences* 68: 15.

Fu, D. (2013). The 2012 stock assessment of paua (*Haliotis iris*) for PAU 5D. *New Zealand Fisheries Assessment Report 2012/xx*. xx p.

Fu, D. (2012). The 2011 stock assessment of paua (*Haliotis iris*) for PAU 7. *New Zealand Fisheries Assessment Report 2012/27*. 56 p.

Fu, D.; McKenzie, A. (2010a). The 2010 stock assessment of paua (*Haliotis iris*) for Chalky and South Coast in PAU 5A. *New Zealand Fisheries Assessment Report 2010/36.* 63 p.

Fu, D.; McKenzie, A. (2010b). The 2010 stock assessment of paua (*Haliotis iris*) for Milford, George, Central, and Dusky in PAU 5A. *New Zealand Fisheries Assessment Report 2010/46*. 55 p.

Gorfine, H.K.; Dixon, C.D. (2000). A behavioural rather than resource-focused approach may be needed to ensure sustainability of quota managed abalone fisheries. *Journal of Shellfish Research* 19: 515–516.

Kim, S.W.; Bentley, N.; Starr, P.J.; Breen, P.A. (2004). Assessment of red rock lobsters (*Jasus edwardsii*) in CRA 4 and CRA 5 in 2003. *New Zealand Fisheries Assessment Report 2004/8*. 165 p.

McShane, P.E.; Mercer, S.F.; Naylor, J.R. (1994). Spatial variation and commercial fishing of the New Zealand paua (*Haliotis iris* and *H. australis*). *New Zealand Journal of Marine and Freshwater Research* 28: 345–355.

McShane, P.E.; Mercer, S.; Naylor, J.R.; Notman, P.R. (1996): Paua (*Haliotis iris*) fishery assessment in PAU 5, 6, and 7. New Zealand Fisheries Assessment Research Document 96/11. 35 p. (Unpublished report held in NIWA library, Wellington.)

McKenzie, A.; Smith, A.N.H. (2009). The 2008 stock assessment of paua (*Haliotis iris*) in PAU 7. *New Zealand Fisheries Assessment Report 2009/34*. 84 p.

Punt, A.E. (2003). The performance of a size-structured stock assessment method in the face of spatial heterogeneity in growth. *Fisheries Research 65:* 391–409.

Schiel, D.R. (1989). Paua fishery assessment 1989. New Zealand Fisheries Assessment Research Document 89/9: 20 p. (Unpublished report held in NIWA library, Wellington, New Zealand.)

Schiel, D.R. (1992). The paua (abalone) fishery of New Zealand. *In:* Abalone of the world: Biology, fisheries and culture. Shepherd, S.A.; Tegner, M.J.; Guzman del Proo, S. (eds.) pp. 427–437. Blackwell Scientific, Oxford.

Schiel, D.R.; Breen, P.A. (1991). Population structure, ageing and fishing mortality of the New Zealand abalone *Haliotis iris*. *Fishery Bulletin 89*: 681–691.

Shepherd, S.A.; Breen, P.A. (1992). Mortality in abalone: its estimation, variability and causes. *In*: 'Abalone of the World: Biology, Fisheries and Culture'. (Eds. Shepherd, S.A.; Tegner, M.J.; Guzman del Proo, S.) pp. 276–304. (Blackwell Scientific: Oxford.)

Shepherd, S.A.; Partington, D. (1995). Studies on Southern Australian abalone (genus Haliotis). XVI. Recruitment, habitat and stock relations. *Marine and Freshwater Research 46*: 669–680.

Shepherd, S.A.; Rodda, K.R.; Vargas, K.M. (2001). A chronicle of collapse in two abalone stocks with proposals for precautionary management. *Journal of Shellfish Research 20:* 843–856.

Table 1: Observed cv and model weighted CV for the PAU 5D CPUE indices for 1990 to 2001 and for 2002 to 2012 from the base case model (5.2).

Fishing Year	Observational CV	Model 5.2 CV	Fishing Year	Observational CV	Model 5.2 CV
1990	0.08	0.12	2002	0.05	0.09
1991	0.07	0.10	2003	0.05	0.09
1992	0.06	0.09	2004	0.05	0.09
1993	0.06	0.08	2005	0.04	0.09
1994	0.06	0.08	2006	0.05	0.10
1995	0.06	0.08	2007	0.05	0.10
1996	0.05	0.08	2008	0.05	0.11
1997	0.05	0.07	2009	0.06	0.11
1998	0.05	0.07	2010	0.06	0.11
1999	0.06	0.08	2011	0.06	0.11
2000	0.05	0.08	2012	0.05	0.11
2001	0.06	0.08			

Table 2: Base case model specifications: for estimated parameters, the phase of estimation, type of prior, (U, uniform; N, normal; LN, lognormal), mean and CV of the prior, lower bound and upper bound.

Parameter	Phase	Prior	μ	CV	Bounds	
					Lower	Upper
ln($R0$)	1	U	–	–	5	50
M	3	LN	0.1	0.35	0.01	0.5
g_1	2	U	–	–	1	50
$g2$	2	U	–	–	0.01	50
φ	2	U	–	–	0.001	1
$Ln(q^I)$	1	U	–	–	-30	0
$Ln(q^J)$	1	U	–	–	-30	0
$Ln(q^k)$	1	U	–	–	-30	0
L_{50}	1	U	–	–	70	145
L_{95-50}	1	U	–	–	1	50
T_{50}	2	U	–	–	70	125
T_{95-50}	2	U	–	–	0.001	50
D_{50}	2	U	–	–	70	145
D_{95-50}	2	U	–	–	0.01	50
ε	1	N	0	0.4	-2.3	2.3
h	1	U	–	–	0.01	2

Table 3: Values for fixed quantities for base case model.

Variable	Value
L_1	75
L_2	120
a	2.99E-08
b	3.303
U^{max}	0/80
σ_{min}	1
σ_{obs}	0.25
$\tilde{\sigma}$	0.2
H	0.75

Table 4: Actual sample sizes, initial sample sizes determined for the multinomial likelihood, and model weighted sample sizes for the PAU 5D commercial catch sampling length frequencies from base case model (5.2).

Fishing year	Actual sample size	Initial sample size	Model 5.2 sample size
1998	2206	476	29
2002	5245	889	54
2003	5907	879	54
2004	3277	675	41
2007	2060	624	38
2008	1378	506	31
2009	3270	798	49
2010	3618	811	49
2011	1707	458	28

Table 5: Summary descriptions for MPD base case and sensitivity runs.

Model	Description
5.2 (base case)	Excluded RDSI and RDLF, included the recent CSLF, TA1.8 weighting method
5.3	5.2, dropped tag-recapture data
5.4	5.2, dropped CSLF
5.5	5.2, dropped the early CPUE series
5.6	5.2, dropped the recent CPUE series
6.3	5.2, fixing growth g_α= 32.5 and g_β = 10
6.4	5.2, fixing growth g_α= 35 and g_β = 12.5
6.5	5.2, fixing growth g_α= 24.5 and g_β = 5
6.6	5.2, fixing growth g_α= 20.5 and g_β = 2.5
7.2	5.2, recreational and illegal catch assumed to increase from 2 to 30 t 1974 to 2012
8.2	5.2, fixing *M* at 0.1
9.2	5.2, fixing CPUE shape parameter at 0.4
9.3	5.2, fixing CPUE shape parameter at 0.8

Table 6:MPD estimates for base case and sensitivity trials. Red indicates parameter fixed and likelihood contributions not used when datasets were removed. SDNRs for CSLF were calculated from mean length for runs using TA.18 weighting method.

	Model Run										
	5.2	5.3	5.4	5.5	5.6	6.3	6.5	7.2	8.2	9.2	9.3
Likelihoods											
CPUE	-11.2	-14.1	-10.0	72.9	-11.4	-12.1	-9.2	-10.6	-0.9	-9.5	-10.1
PCPUE	-9.4	-12.0	-9.9	-9.4	71.0	-9.8	-6.7	-9.4	-7.5	-8.1	-9.5
RDSI	–	–	–	–	–	–	–	–	–	–	–
CSLF	7.8	10.1	127.8	9.1	7.3	9.4	8.9	8.2	16.9	6.1	7.4
RDLF	–	–	–	–	–	–	–	–	–	–	–
Tags	664.4	797.5	664.1	664.2	664.2	703.4	763.1	664.5	667.6	664.2	664.4
Maturity	-33.4	-33.4	-33.4	-33.4	-33.4	-33.4	-33.4	-33.4	-33.4	-33.4	-33.4
Prior on *M*	6.9	1.9	-1.1	0.7	4.5	12.1	1.4	8.4	0.0	2.0	5.7
Prior on ε	-2,416	-2,417	-2,421	-2,421	-2,418	-2,414	-2,420	-2,415	-2,409	-2,420	-2,418
U penalty	0.0	0.0	0.0	0.0	0.0	0.0	0.0	0.0	0.0	0.0	0.0
ε penalty	0.0	0.0	0.0	0.0	0.0	0.0	0.0	0.0	0.0	0.0	0.0
Total	-1,791	-2,464	-1,812	-1,790	-1,787	-2,448	-2,459	-1,788	-1,766	-1,799	-1,793
Parameters											
ln(*R0*)	13.77	13.73	13.96	13.60	13.67	13.65	14.11	13.94	13.46	13.67	13.75
M	0.150	0.129	0.108	0.123	0.141	0.168	0.127	0.156	0.100	0.130	0.146
T_{50}	79.4	79.4	79.4	79.4	79.4	79.4	79.4	79.4	79.4	79.4	79.4
T_{95-50}	13.7	13.7	13.7	13.7	13.7	13.8	13.7	13.7	13.8	13.7	13.7
D_{50}	123.0	122.7	123.0	123.3	123.4	123.0	122.8	123.0	122.4	123.2	123.0
D_{95-50}	4.3	4.9	4.3	4.6	4.7	4.2	4.2	4.3	3.8	4.5	4.3
L_{50}	–	–	–	–	–	–	–	–	–	–	–
L_{95-50}	–	–	–	–	–	–	–	–	–	–	–
$\ln(q^{I})$	-13.0	-13.4	-14.6	-13.0	-13.0	-12.6	-13.8	-13.2	-13.3	-5.3	-10.4
$\ln(q^{I2})$	-12.8	-13.4	-14.6	-12.6	-12.8	-12.2	-13.8	-13.0	-13.0	-5.1	-10.2
$\ln(q^{J})$	–	–	–	–	–	–	–	–	–	–	–

h	1.00	1.00	1.00	1.00	1.00	1.00	1.00	1.00	1.00	0.40	0.80
g_α	28.60	42.93	27.65	28.26	27.65	32.50	24.50	28.70	30.23	28.03	28.59
g_β	7.46	4.35	7.68	7.57	7.52	10.00	5.00	7.46	7.05	7.55	7.46
φ	0.42	0.42	0.42	0.42	0.42	0.42	0.42	0.42	0.42	0.42	0.42
Indicators											
B_0	2237	2418	4386	2543	2214	1968	3261	2527	2888	2530	2300
$B_{current}$	736	1097	2894	612	492	425	1868	900	714	768	751
$B_{current}/B_0$	0.33	0.45	0.66	0.24	0.22	0.22	0.57	0.36	0.25	0.30	0.33
rB_0	1906	2125	3948	2248	1903	1753	2565	2137	2621	2213	1971
$rB_{current}$	457	835	2476	381	255	263	1225	562	503	505	475
$rB_{current}/rB_0$	0.24	0.39	0.63	0.17	0.13	0.15	0.48	0.26	0.19	0.23	0.24
$U_{current}$	0.23	0.13	0.04	0.28	0.41	0.38	0.09	0.26	0.21	0.21	0.23
Weights											
CPUE	0.15	0.15	0.15	0.15	0.15	0.15	0.15	0.15	0.15	0.15	0.15
PCPUE	0.10	0.10	0.10	0.10	0.10	0.10	0.10	0.10	0.10	0.10	0.10
RDSI	–	–	–	–	–	–	–	–	–	–	–
CSLF	0.01	0.01	0.01	0.01	0.01	0.01	0.01	0.01	0.01	0.01	0.01
RDLF	–	–	–	–	–	–	–	–	–	–	–
Tags	0.20	0.20	0.20	0.20	0.20	0.20	0.20	0.20	0.20	0.20	0.20
Maturity	3.93	3.93	3.93	3.93	3.93	3.93	3.93	3.93	3.93	3.93	3.93
sdnrs											
CPUE	1.17	0.94	1.25	3.34	1.16	1.11	1.30	1.21	1.75	1.29	1.25
PCPUE	1.03	0.75	0.97	1.02	2.74	0.99	1.24	1.02	1.18	1.13	1.01
RDSI	–	–	–	–	–	–	–	–	–	–	–
CSLF	1.00	1.11	0.84	1.33	1.08	1.14	1.07	1.00	1.00	1.02	1.00
RDLF	–	–	–	–	–	–	–	–	–	–	–
Tags	1.19	1.91	1.17	1.18	1.19	0.92	1.66	1.19	1.25	1.18	1.19
Maturity	1.00	1.00	1.00	1.00	1.00	1.00	1.00	1.00	1.00	1.00	1.00

Table 7: Summary of the marginal posterior distributions from the MCMC chain from the base case (5.2). The columns show the minimum values observed in the 1000 samples, the maxima, the 5th and 95th percentiles, and the medians. Biomass is in tonnes.

	Min	5%	Median	95%	Max
Parameters					
f	-1784.9	-1778.3	-1772.0	-1763.5	-1751.3
ln(*R0*)	13.6	13.7	13.8	13.9	14.1
M	0.119	0.134	0.149	0.167	0.192
D_{50}	120.7	121.8	122.8	123.7	125.3
$D_{95\text{-}50}$	0.3	2.8	4.3	6.2	8.5
L_{50}	76.4	78.2	79.3	80.4	81.5
$L_{95\text{-}50}$	7.5	11.2	13.9	17.0	20.7
$\ln(q^I)$	-13.6	-13.3	-13.1	-12.9	-12.7
$\ln(q^{II})$	-13.7	-13.2	-12.9	-12.6	-12.2
g_α	23.0	26.4	29.3	32.5	36.7
g_β	6.6	7.0	7.4	7.8	8.3
Indicators					
B_0	1928	2099	2285	2487	2852
B_{msy}	507	569	624	684	770
$B_{current}$	504	640	795	1028	1686
$B_{current}/B_0$	0.24	0.28	0.35	0.44	0.60
$B_{current}/B_{msy}$	0.87	1.03	1.28	1.61	2.24
B_0^r	1575	1760	1954	2158	2492
B_{msy}^r	222	297	361	427	498
$B_{current}^r$	277	387	514	710	1299
$B_{current}^r/B_0^r$	0.16	0.20	0.26	0.35	0.54
$B_{current}^r/B_{msy}^r$	0.80	1.05	1.43	2.02	3.08
MSY	110	115	121	130	155
U_{msy}	0.19	0.22	0.26	0.32	0.41
$U_{\%40B_0}$	0.12	0.14	0.16	0.18	0.23
$U_{current}$	0.09	0.15	0.21	0.27	0.39

Table 8: Summary of the marginal posterior distributions from the MCMC chain from the model 5.5. The columns show the minimum values observed in the 1000 samples, the maxima, the 5th and 95th percentiles, and the medians. Biomass is in tonnes.

	Min	5%	Median	95%	Max
Parameters					
f	-1782.9	-1777.6	-1771.3	-1763.2	-1744.8
ln(*R0*)	13.4	13.5	13.6	13.7	13.9
M	0.096	0.110	0.125	0.142	0.164
D_{50}	121.2	122.1	123.1	124.2	125.6
$D_{95\text{-}50}$	1.5	3.1	4.8	6.7	9.8
L_{50}	76.8	78.2	79.3	80.4	81.7
$L_{95\text{-}50}$	8.5	11.3	14.0	17.0	23.1
$\ln(q^{I})$	–	–	–	–	–
$\ln(q^{II})$	-13.3	-12.9	-12.7	-12.4	-12.1
g_{α}	23.1	26.1	29.1	32.7	36.5
g_{β}	6.8	7.1	7.5	7.9	8.3
Indicators					
B_0	2119	2335	2535	2742	2977
B_{msy}	557	640	704	771	857
$B_{current}$	420	524	647	814	1132
$B_{current} / B_0$	0.16	0.20	0.26	0.32	0.42
$B_{current} / B_{msy}$	0.57	0.73	0.92	1.18	1.55
B_0^r	1820	2025	2241	2469	2741
B_{msy}^r	314	390	467	550	664
$B_{current}^r$	254	318	414	548	840
$B_{current}^r / B_0^r$	0.11	0.14	0.19	0.25	0.35
$B_{current}^r / B_{msy}^r$	0.47	0.64	0.89	1.26	1.94
MSY	103	108	113	120	132
U_{msy}	0.14	0.17	0.20	0.24	0.30
$U_{\%40B_0}$	0.09	0.11	0.13	0.15	0.18
$U_{current}$	0.13	0.20	0.26	0.33	0.42

Table 9: Summary of the marginal posterior distributions from the MCMC chain from the model 6.3. The columns show the minimum values observed in the 1000 samples, the maxima, the 5th and 95th percentiles, and the medians. Biomass is in tonnes.

	Min	5%	Median	95%	Max
Parameters					
f	-2441.0	-2435.8	-2429.4	-2421.5	-2408.4
ln(*R0*)	13.5	13.6	13.6	13.7	13.8
M	0.134	0.150	0.167	0.186	0.215
D_{50}	120.7	121.9	122.8	123.8	124.9
$D_{95\text{-}50}$	0.8	2.7	4.3	6.2	9.4
L_{50}	76.8	78.2	79.3	80.4	81.6
$L_{95\text{-}50}$	7.7	11.2	14.0	17.1	23.8
$\ln(q^{I})$	-13.01	-12.86	-12.70	-12.53	-12.31
$\ln(q^{II})$	-12.8	-12.5	-12.3	-12.1	-11.8
g_{α}	32.5	32.5	32.5	32.5	32.5
g_{β}	10.0	10.0	10.0	10.0	10.0
Indicators					
B_0	1631	1821	1987	2158	2345
B_{msy}	451	506	556	609	673
$B_{current}$	325	379	444	526	660
$B_{current} / B_0$	0.15	0.19	0.22	0.27	0.35
$B_{current} / B_{msy}$	0.55	0.66	0.80	0.97	1.27
B_0^r	1397	1596	1772	1951	2146
B_{msy}^r	263	327	385	443	514
$B_{current}^r$	183	225	279	352	465
$B_{current}^r / B_0^r$	0.10	0.13	0.16	0.20	0.27
$B_{current}^r / B_{msy}^r$	0.44	0.56	0.73	0.96	1.41
MSY	113	116	119	122	127
U_{msy}	0.19	0.22	0.25	0.29	0.36
$U_{\%40B_0}$	0.13	0.14	0.16	0.19	0.22
$U_{current}$	0.22	0.29	0.35	0.43	0.55

Table 10: Summary of the marginal posterior distributions from the MCMC chain from model 6.5. The columns show the minimum values observed in the 1000 samples, the maxima, the 5th and 95th percentiles, and the medians. Biomass is in tonnes.

	Min	5%	Median	95%	Max
Parameters					
f	-2452.7	-2446.9	-2440.5	-2432.9	-2421.4
ln(*R0*)	13.7	14.0	14.2	14.4	14.9
M	0.098	0.113	0.128	0.144	0.169
D_{50}	120.7	121.8	122.8	123.7	125.0
$D_{95\text{-}50}$	1.1	2.9	4.4	6.2	8.5
L_{50}	76.5	78.2	79.3	80.4	81.8
$L_{95\text{-}50}$	8.4	11.3	13.9	17.1	22.8
$\ln(q^{I})$	-14.61	-14.16	-13.90	-13.67	-13.38
$\ln(q^{II})$	-14.7	-14.2	-13.9	-13.6	-13.3
g_{α}	24.5	24.5	24.5	24.5	24.5
g_{β}	5.0	5.0	5.0	5.0	5.0
Indicators					
B_0	2733	3053	3375	3841	4839
B_{msy}	742	825	912	1036	1307
$B_{current}$	1177	1576	2015	2702	4133
$B_{current} / B_0$	0.37	0.50	0.60	0.72	0.86
$B_{current} / B_{msy}$	1.34	1.85	2.21	2.66	3.20
B_0^r	1987	2358	2650	3021	3709
B_{msy}^r	144	257	342	434	543
$B_{current}^r$	711	1002	1339	1863	2947
$B_{current}^r / B_0^r$	0.30	0.41	0.51	0.64	0.82
$B_{current}^r / B_{msy}^r$	1.68	2.81	3.91	5.82	11.65
MSY	113	136	156	189	289
U_{msy}	0.19	0.24	0.31	0.41	0.65
$U_{\%40B_0}$	0.11	0.13	0.16	0.20	0.29
$U_{current}$	0.04	0.06	0.08	0.11	0.16

Table 11: Summary of key indicators from the projection for the base case (5.2) MCMC with future commercial catch set to current TACC and non-commercial catch set to 20 t: projected biomass as a percentage of the virgin and current stock status, for spawning stock and recruit-sized biomass.

Projection under	2012	2013	2014	2015
$\%B_0$	0.349(0.275–0.456)	0.361(0.276–0.482)	0.374(0.274–0.513)	0.388(0.273–0.538)
$\%B_{msy}$	1.276(0.999–1.687)	1.32(1.00–1.78)	1.368(0.991–1.893)	1.419(0.988–1.987)
$\Pr(> B_{msy})$	0.974	0.976	0.971	0.972
$\Pr(> B_{current})$		0.658	0.738	0.791
$\Pr(> 40\%B_0)$	0.152	0.235	0.331	0.426
$\Pr(< 20\%B_0)$	0.000	0.000	0.000	0.000
$\Pr(< 10\%B_0)$	0.000	0.000	0.000	0.000
$\%B_0^r$	0.264(0.192–0.371)	0.268(0.193–0.377)	0.275(0.197–0.388)	0.287(0.199–0.407)
$\%B_{msy}^r$	1.426(0.992–2.164)	1.45(1.00–2.20)	1.49(1.02–2.26)	1.55(1.02–2.36)
$\Pr(> B_{msy}^r)$	0.973	0.976	0.980	0.981
$\Pr(> B_{current}^r)$	0.000	0.893	0.916	0.846
$\Pr(U_{proj} > U_{40\%B0})$	0.917	0.903	0.885	0.849

Table 12: Summary of key indicators from the projection for MCMC 5.5 with future commercial catch set to current TACC and non-commercial catch set to 20 t: projected biomass as a percentage of the virgin and current stock status, for spawning stock and recruit-sized biomass.

Projection under	2012	2013	2014	2015
$\%B_0$	0.256(0.195–0.342)	0.264(0.194–0.359)	0.272(0.192–0.383)	0.282(0.189–0.403)
$\%B_{msy}$	0.924(0.699–1.246)	0.951(0.697–1.307)	0.981(0.688–1.393)	1.017(0.677–1.471)
$\Pr(> B_{msy})$	0.291	0.379	0.459	0.532
$\Pr(> B_{current})$		0.651	0.717	0.762
$\Pr(> 40\%B_0)$	0.002	0.004	0.011	0.029
$\Pr(< 20\%B_0)$	0.037	0.037	0.038	0.042
$\Pr(< 10\%B_0)$	0.000	0.000	0.000	0.000
$\%B_0^r$	0.185(0.133–0.262)	0.187(0.130–0.269)	0.191(0.130–0.276)	0.198(0.130–0.293)
$\%B_{msy}^r$	0.89(0.61–1.36)	0.90(0.60–1.39)	0.917(0.596–1.424)	0.949(0.592–1.506)
$\Pr(> B_{msy}^r)$	0.282	0.306	0.344	0.414
$\Pr(> B_{current}^r)$	0.000	0.727	0.776	0.760
$\Pr(U_{proj} > U_{40\%B0})$	0.999	0.999	0.999	0.998

Table 13: Summary of key indicators from the projection for MCMC 6.3 with future commercial catch set to current TACC and non-commercial catch set to 20 t: projected biomass as a percentage of the virgin and current stock status, for spawning stock and recruit-sized biomass.

Projection under	2012	2013	2014	2015
$\%B_0$	0.224(0.179–0.282)	0.236(0.177–0.319)	0.250(0.174–0.354)	0.267(0.172–0.395)
$\%B_{msy}$	0.800(0.637–1.014)	0.844(0.632–1.144)	0.893(0.616–1.270)	0.954(0.611–1.418)
$\Pr(> B_{msy})$	0.0324	0.1312	0.2704	0.4088
$\Pr(> B_{current})$		0.6978	0.7776	0.83
$\Pr(> 40\%B_0)$	0	0	0.0046	0.023
$\Pr(< 20\%B_0)$	0.1632	0.1244	0.113	0.0988
$\Pr(< 10\%B_0)$	0	0	0	0.0002
$\%B_0^r$	0.158(0.119–0.212)	0.163(0.120–0.221)	0.173(0.121–0.243)	0.187(0.116–0.284)
$\%B_{msy}^r$	0.731(0.535–1.014)	0.756(0.543–1.058)	0.803(0.544–1.161)	0.867(0.525–1.357)
$\Pr(> B_{msy}^r)$	0.031	0.052	0.126	0.272
$\Pr(> B_{current}^r)$	0.000	0.920	0.849	0.839
$\Pr(U_{proj} > U_{40\%B0})$	1.00	1.00	1.00	1.00

Table 14: Summary of key indicators from the projection for MCMC 6.5 with future commercial catch set to current TACC and non-commercial catch set to 20 t: projected biomass as a percentage of the virgin and current stock status, for spawning stock and recruit-sized biomass.

Projection under	2012	2013	2014	2015
$\%B_0$	0.598(0.486–0.736)	0.608(0.488–0.755)	0.619(0.488–0.784)	0.631(0.489–0.808)
$\%B_{msy}$	2.21(1.79–2.72)	2.25(1.80–2.80)	2.29(1.80–2.91)	2.33(1.80–2.99)
$\Pr(> B_{msy})$	1.000	1.000	1.000	1.000
$\Pr(> B_{current})$	0.000	0.624	0.693	0.740
$\Pr(> 40\%B_0)$	1.000	1.000	1.000	1.000
$\Pr(< 20\%B_0)$	0.000	0.000	0.000	0.000
$\Pr(< 10\%B_0)$	0.000	0.000	0.000	0.000
$\%B_0^r$	0.506(0.388–0.662)	0.507(0.386–0.659)	0.507(0.384–0.659)	0.510(0.386–0.662)
$\%B_{msy}^r$	3.91(2.66–6.26)	3.91(2.64–6.27)	3.91(2.63–6.29)	3.92(2.64–6.32)
$\Pr(> B_{msy}^r)$	1.000	1.000	1.000	1.000
$\Pr(> B_{current}^r)$	0.000	0.439	0.446	0.502
$\Pr(U_{proj} > U_{40\%B0})$	0.001	0.001	0.001	0.001

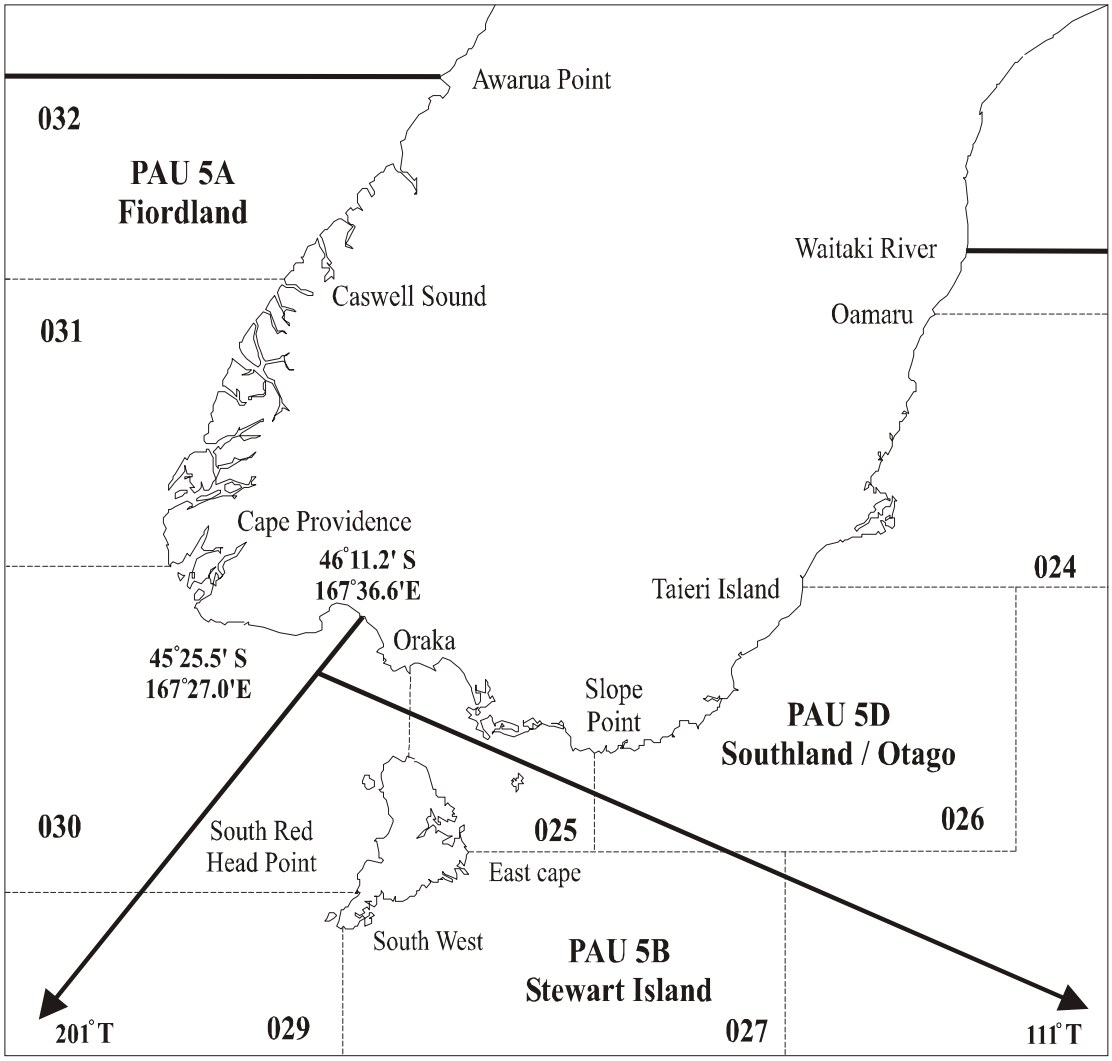

Figure 1: Map of PAU 5 showing the boundaries of the general statistical areas.

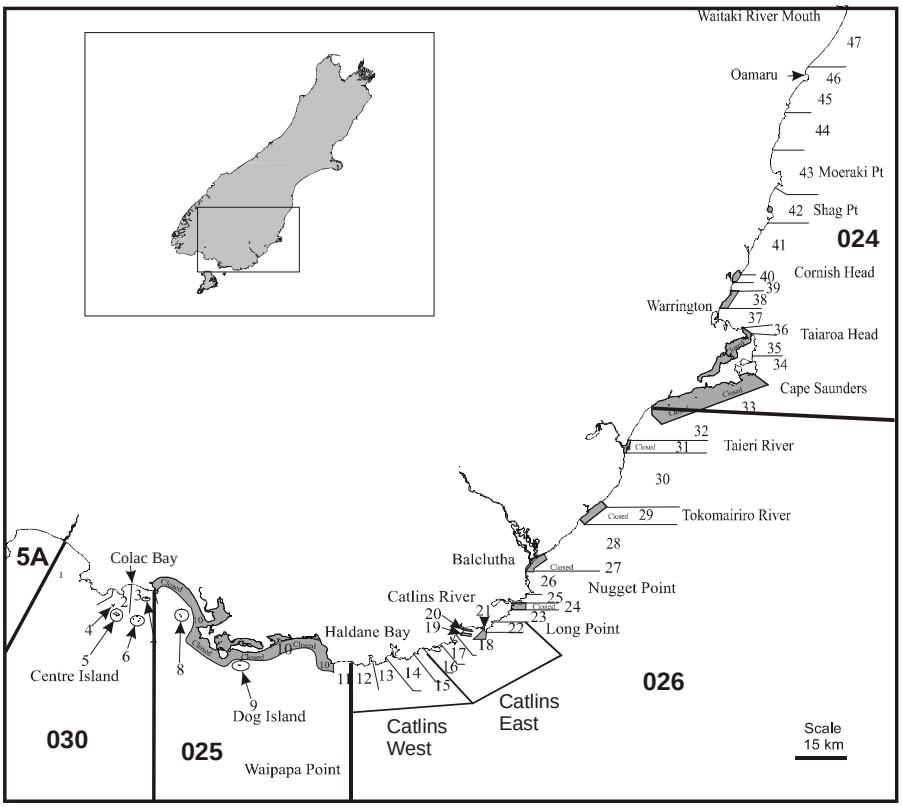

Figure 2: Research survey strata within PAU 5D.

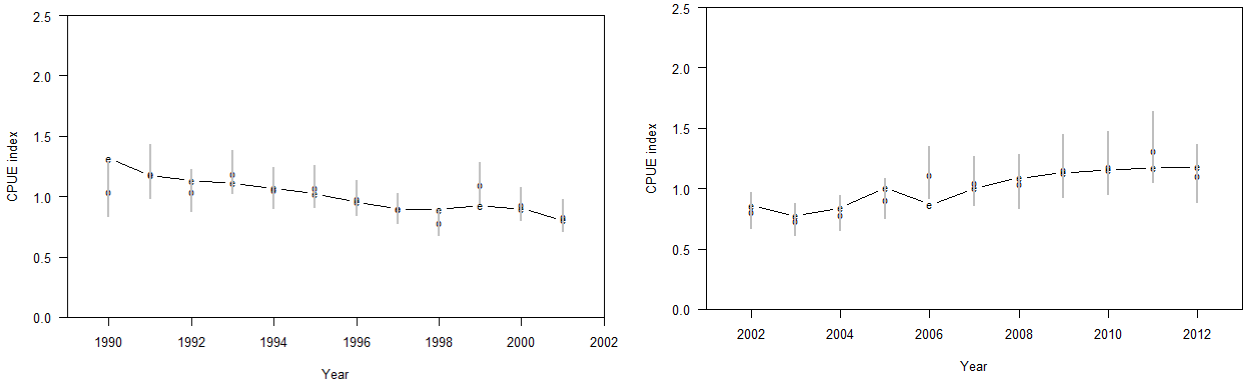

Figure 3: MPD fits to the CPUE indices (left) and PCPUE indices (right), for the base case model (5.2).

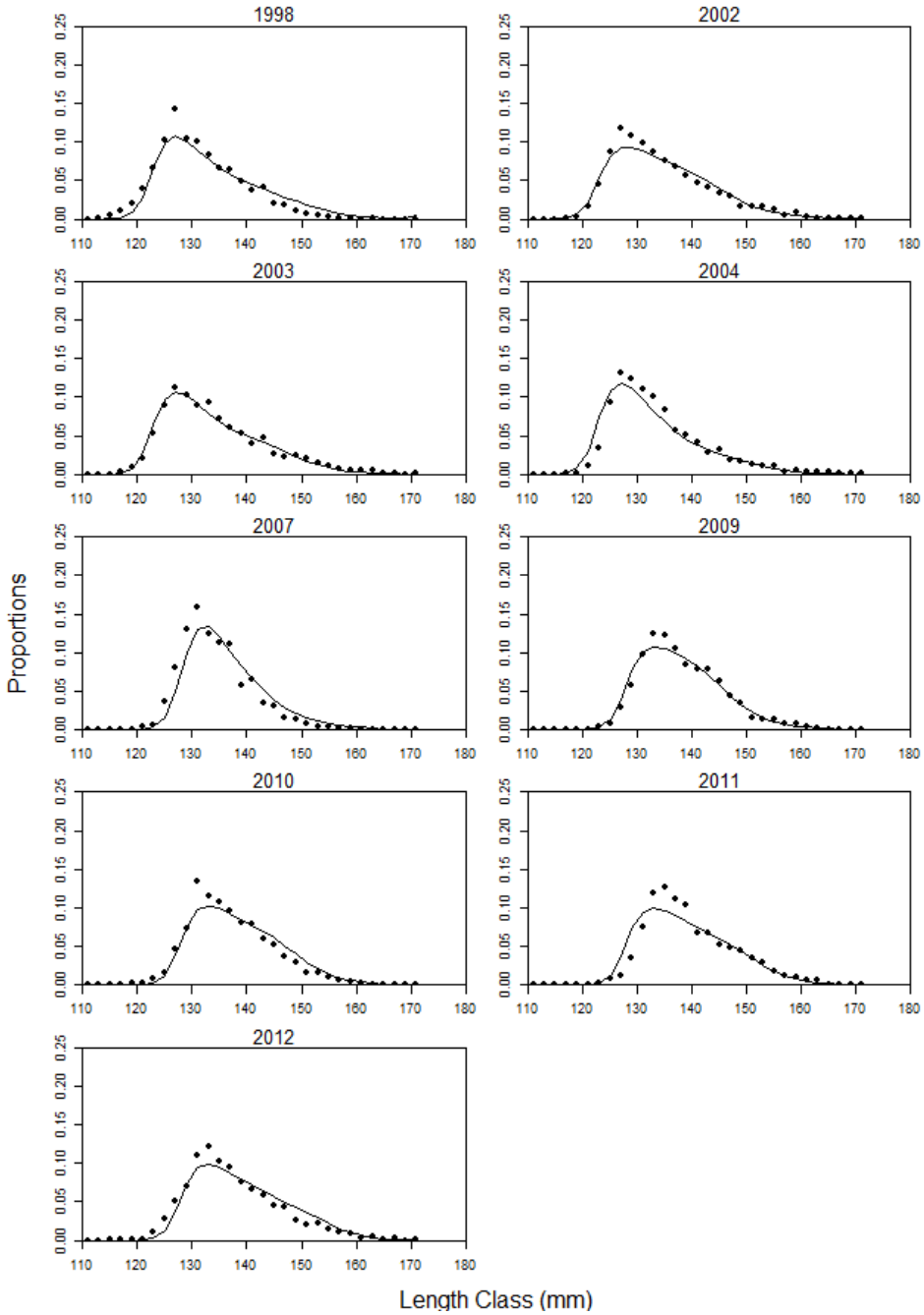

Figure 4: MPD fits to the CSLF data for the base case model (5.2).

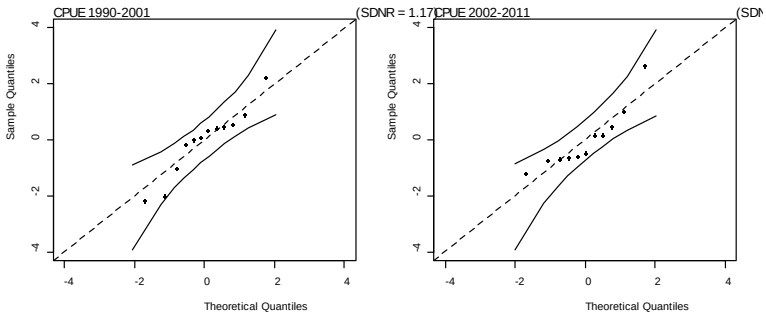

Figure 5: Normal Q-Q plots for residuals from fits to the two CPUE datasets for the MPD base case model (5.2).

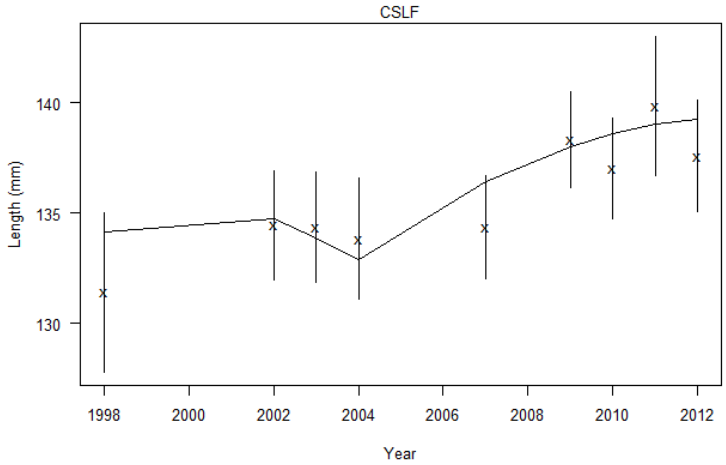

Figure 6: Observed and predicted mean length by year for the CSLF datasets for MPD base case model (5.2). The vertical lines are confidence intervals for the mean length.

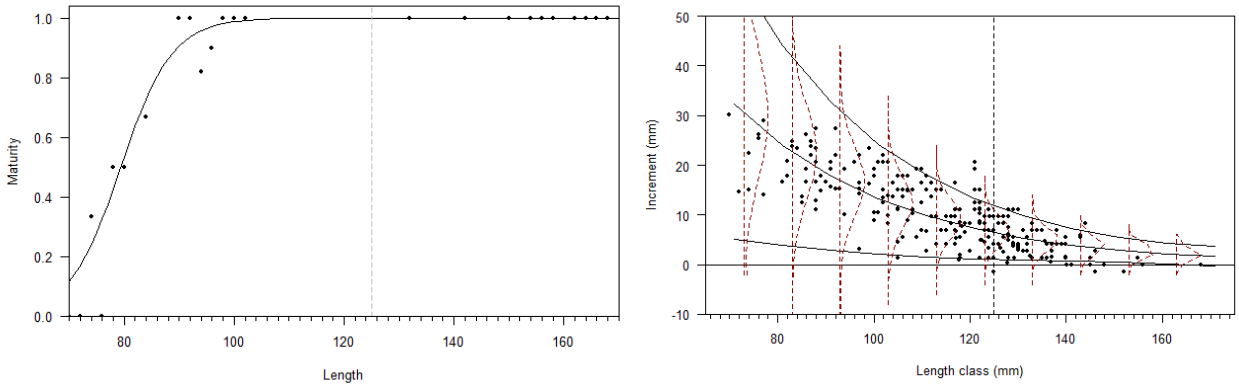

Figure 7: MPD fits to the maturity data (left: dots are observed proportion mature at length with confidence interval; the lines are predicted proportion of maturity at length) and the tag-recapture data (right: The dots are observed mean annual increments; the black lines are the fitted growth curve with 95% confidence intervals; dashed lines are from the estimated growth transition matrix at selected sizes) for base case model (5.2).

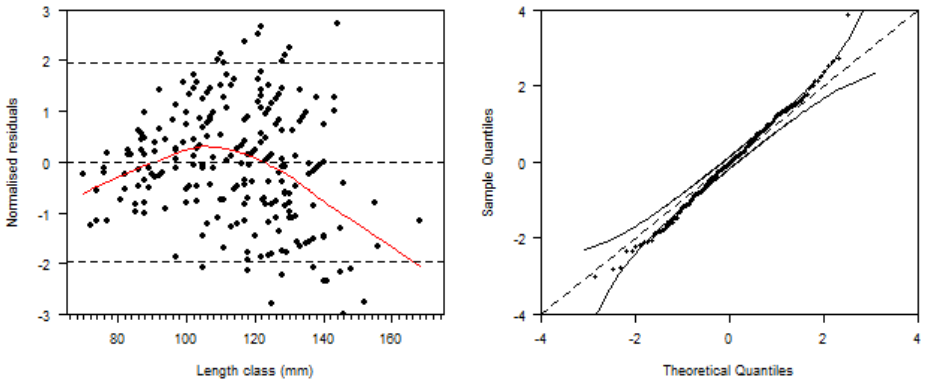

Figure 8: Normalised residuals by length class (left) and Normal Q-Q plot from the fits to the tag-recapture data for the base case model (5.2).

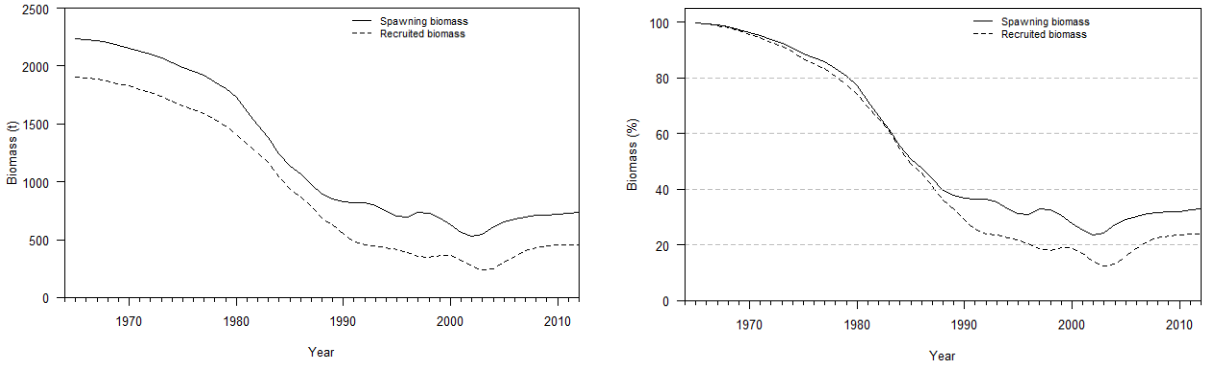

Figure 9: Estimated spawning and recruit-sized biomass (left) and spawning and recruit-sized biomass as a percentage of the virgin level (right) for MPD base case model (5.2).

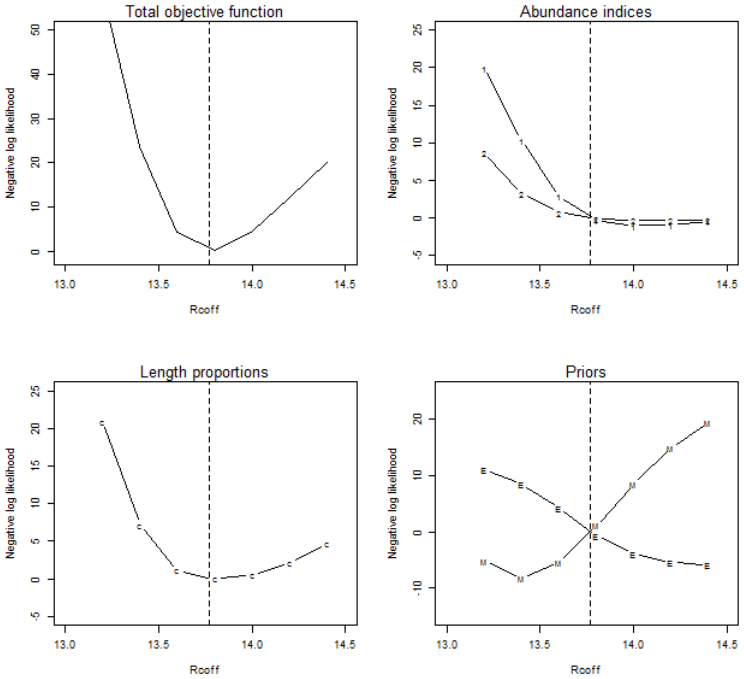

Figure 10: Profile likelihood for parameter $\ln(R0)$ for the base case model (5.2). The profile likelihood is shown for the total objective function value (top left), component likelihood (top right for the CPUE and bottom left for the CSLF), and for the prior (bottom right, E represents prior on the recruitment deviation and *M* represents prior on the natural mortality). Dashed line represents the minimum value.

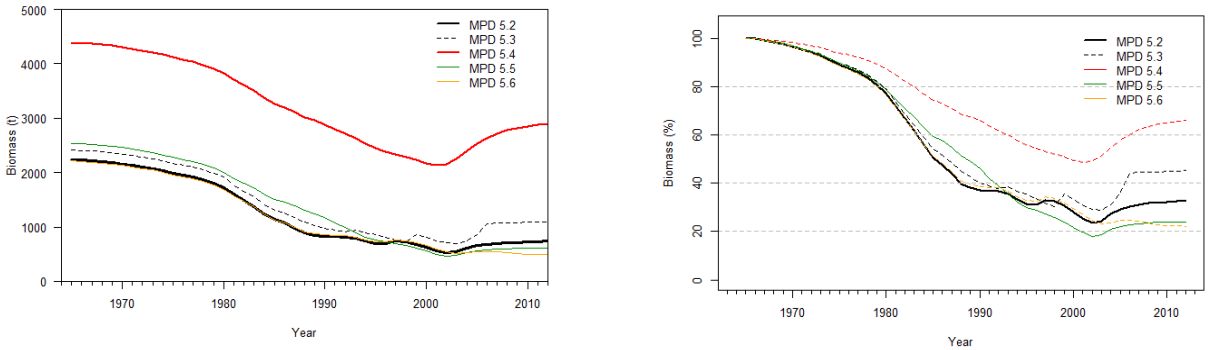

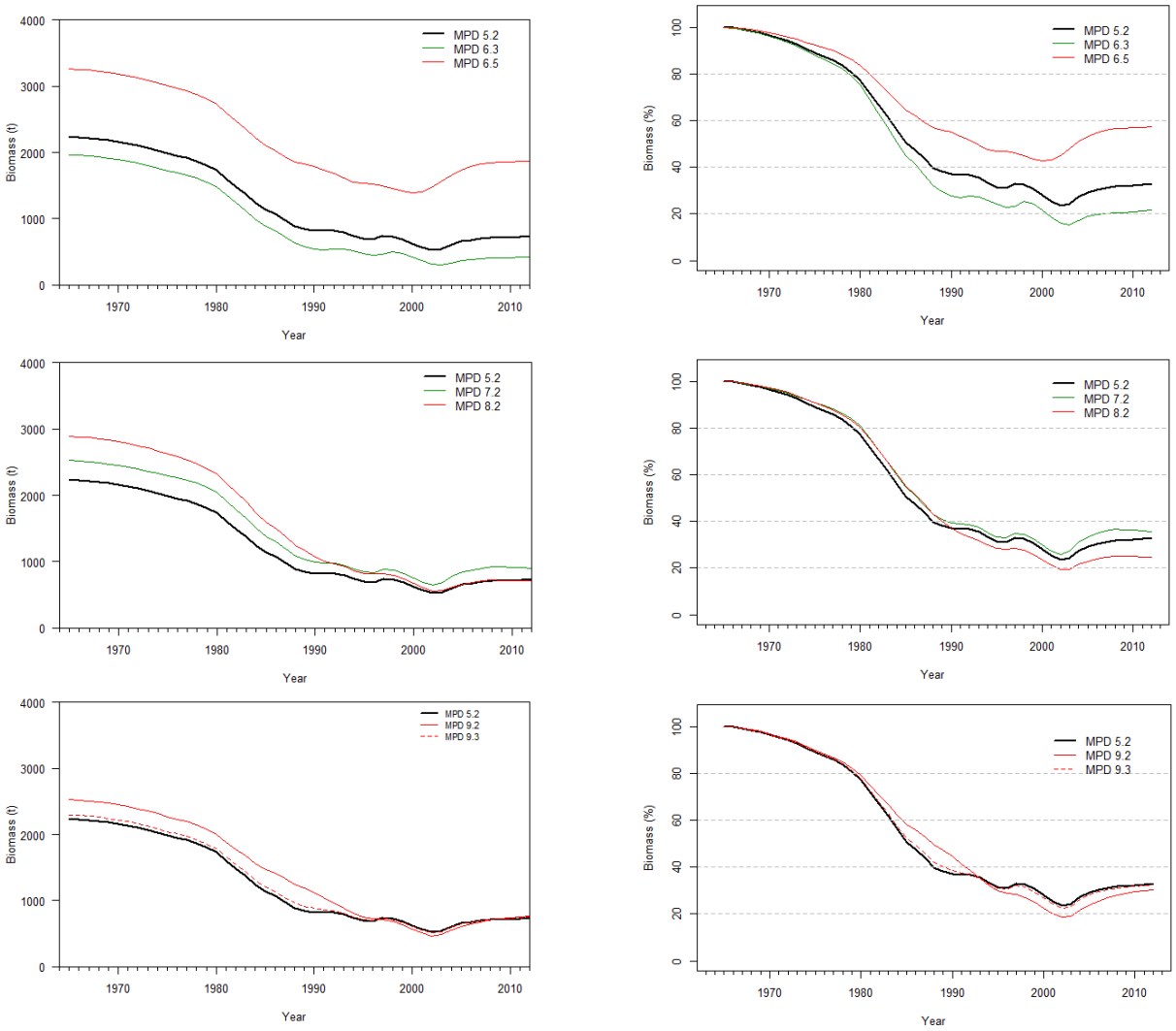

Figure 11: A comparison of Estimated spawning (left) and spawning biomass as a percentage of the virgin level (right) for MPD base case model (5.2) and selected sensitivity model runs. See Table 5 for the description of the sensitivity model runs.

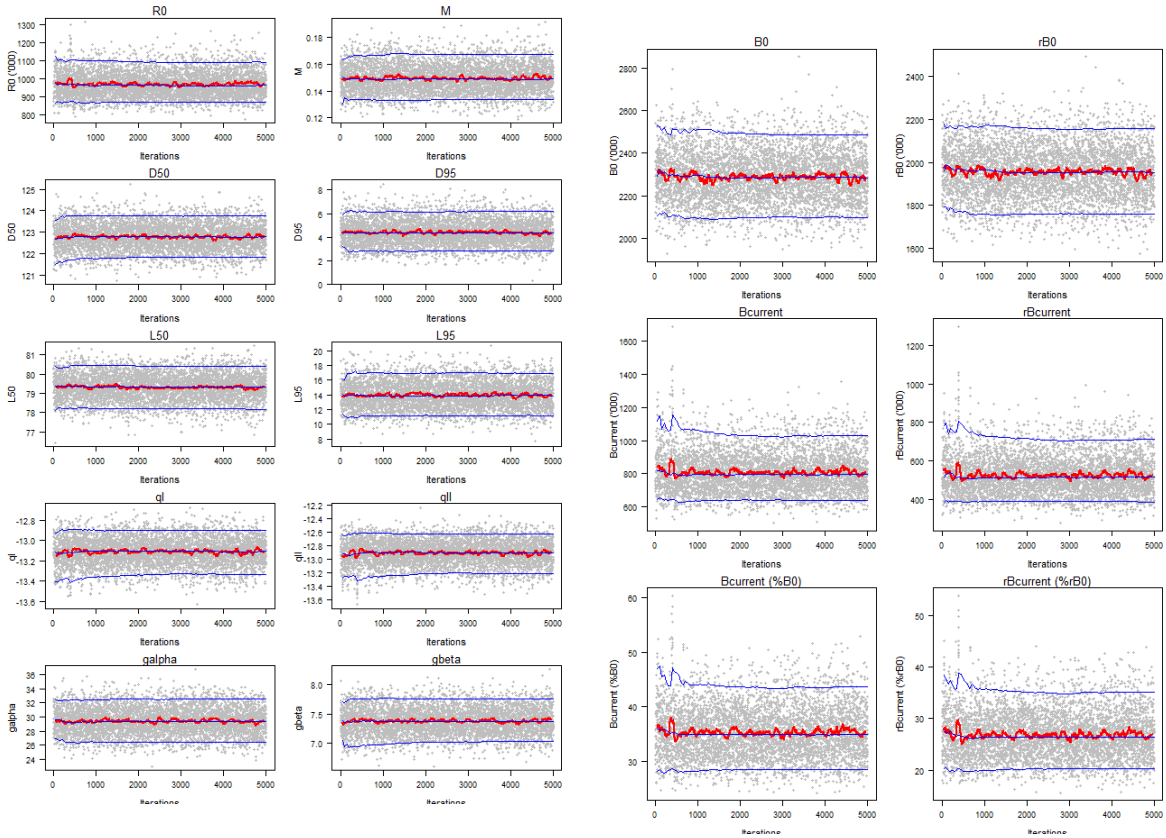

Figure 12: Traces of estimated parameters (left) and biomass indicators (right) for base case MCMC 5.2.

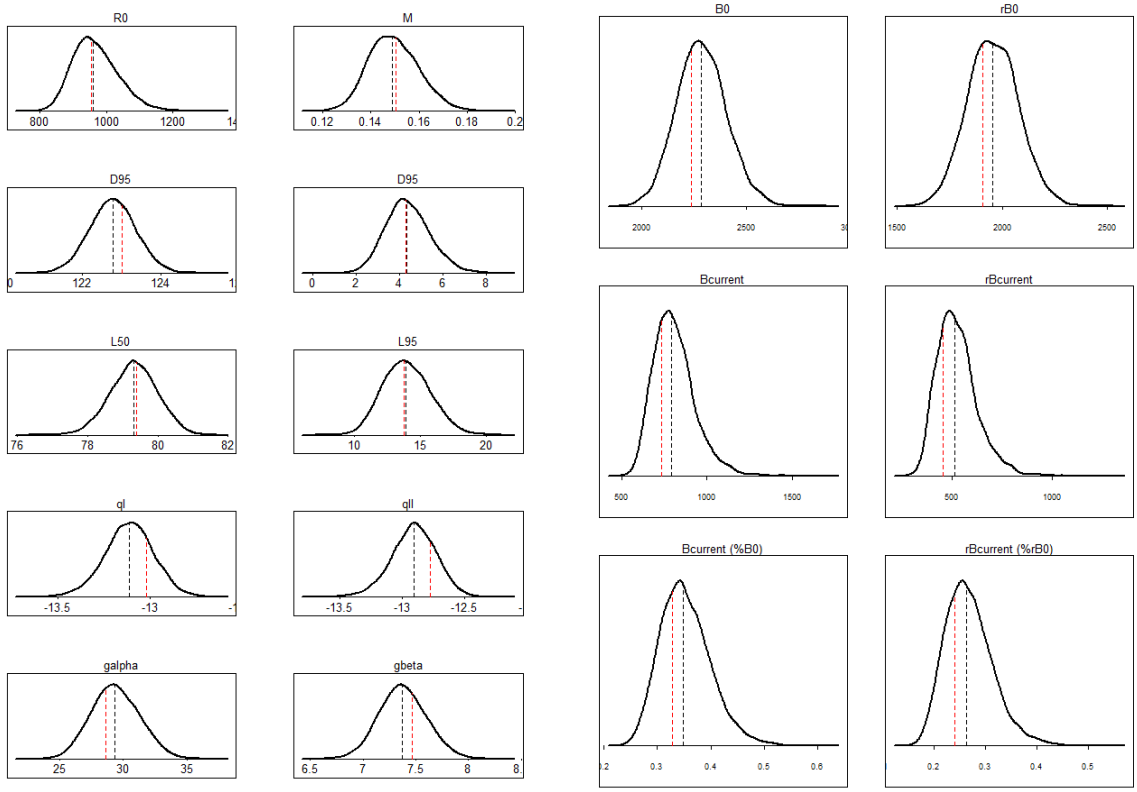

Figure 13: Posterior distributions of estimated parameters (left) and biomass indicators for base case MCMC 5.2 (right). The black dashed lines are the posterior median and red dashed lines are the MPD estimates.

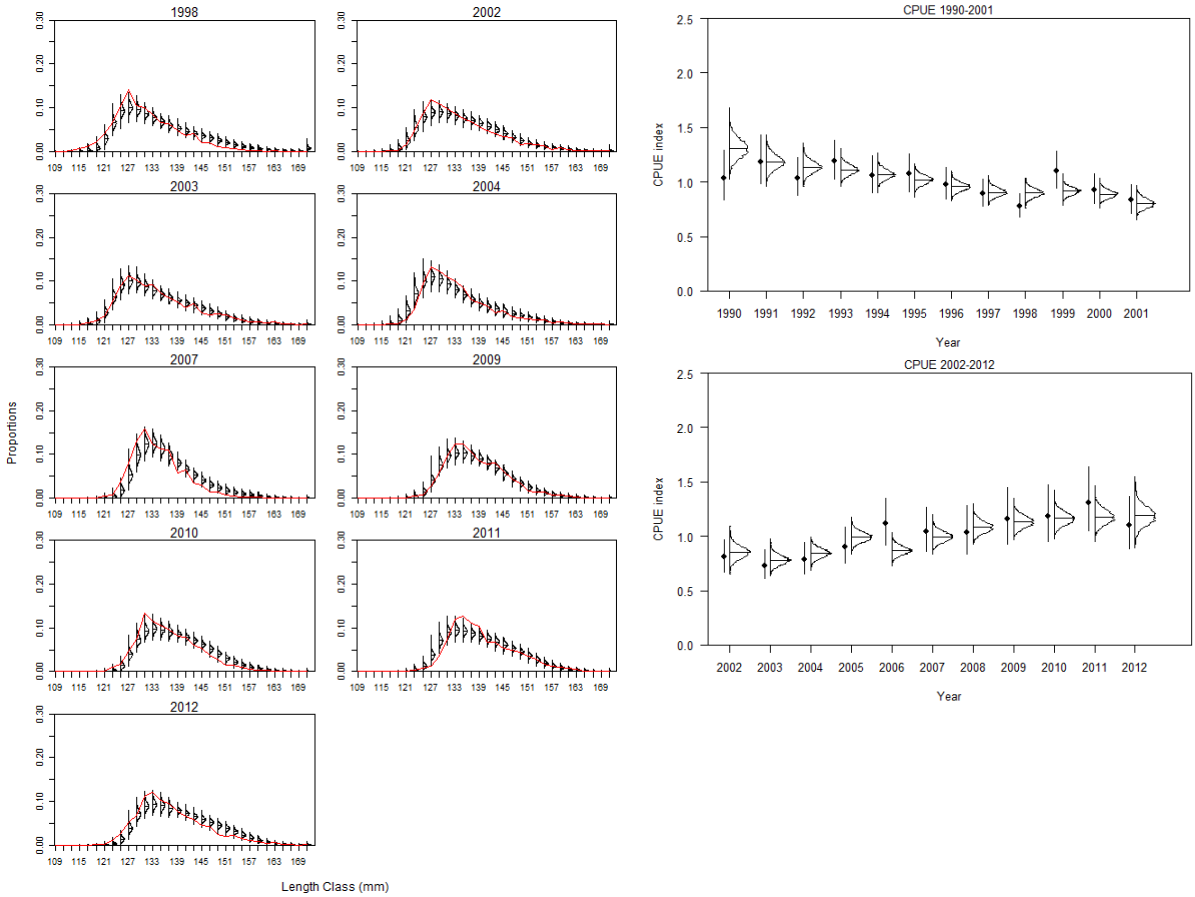

Figure 14: Posterior of the fits to the CSLF (left), and the two CPUE datasets (right) from MCMC 5.2.

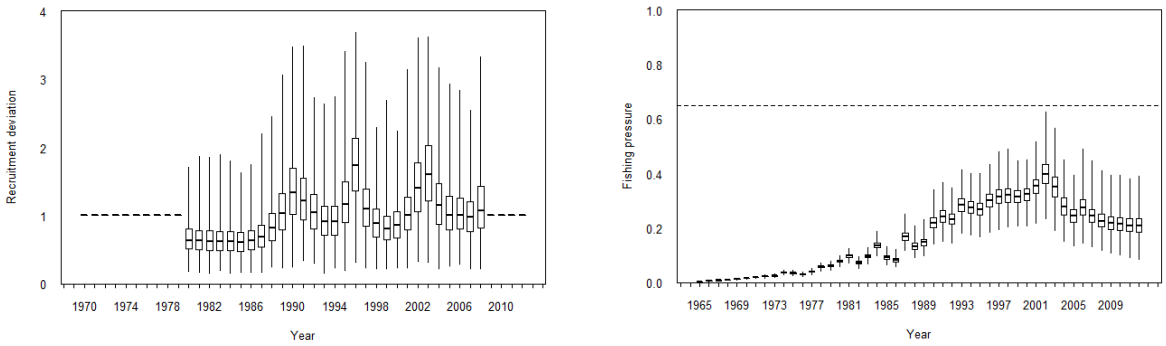

Figure 15: Posterior distributions of recruitment deviations (left), and exploitation rates (right) for the MCMC 5.2 (left). The box shows the median of the posterior distribution (horizontal bar), the 25th and 75th percentiles (box), with the whiskers representing the full range of the distribution. Recruitment deviations were estimated for 1980–2008, and fixed at 1 for other years.

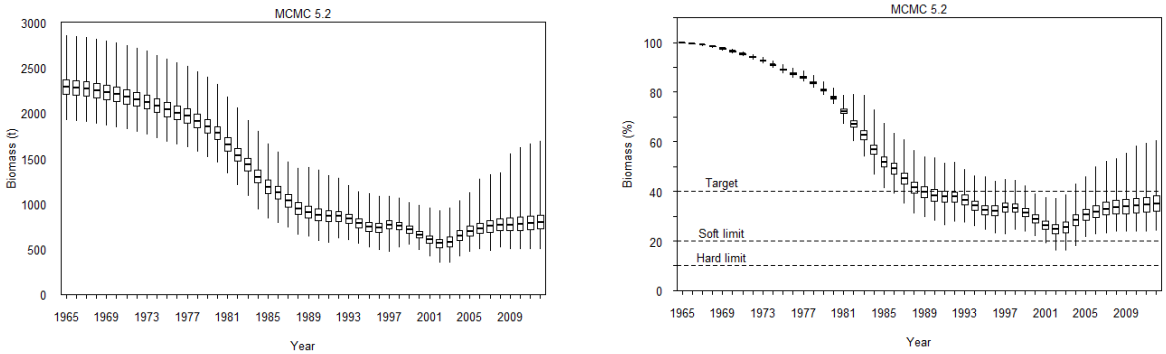

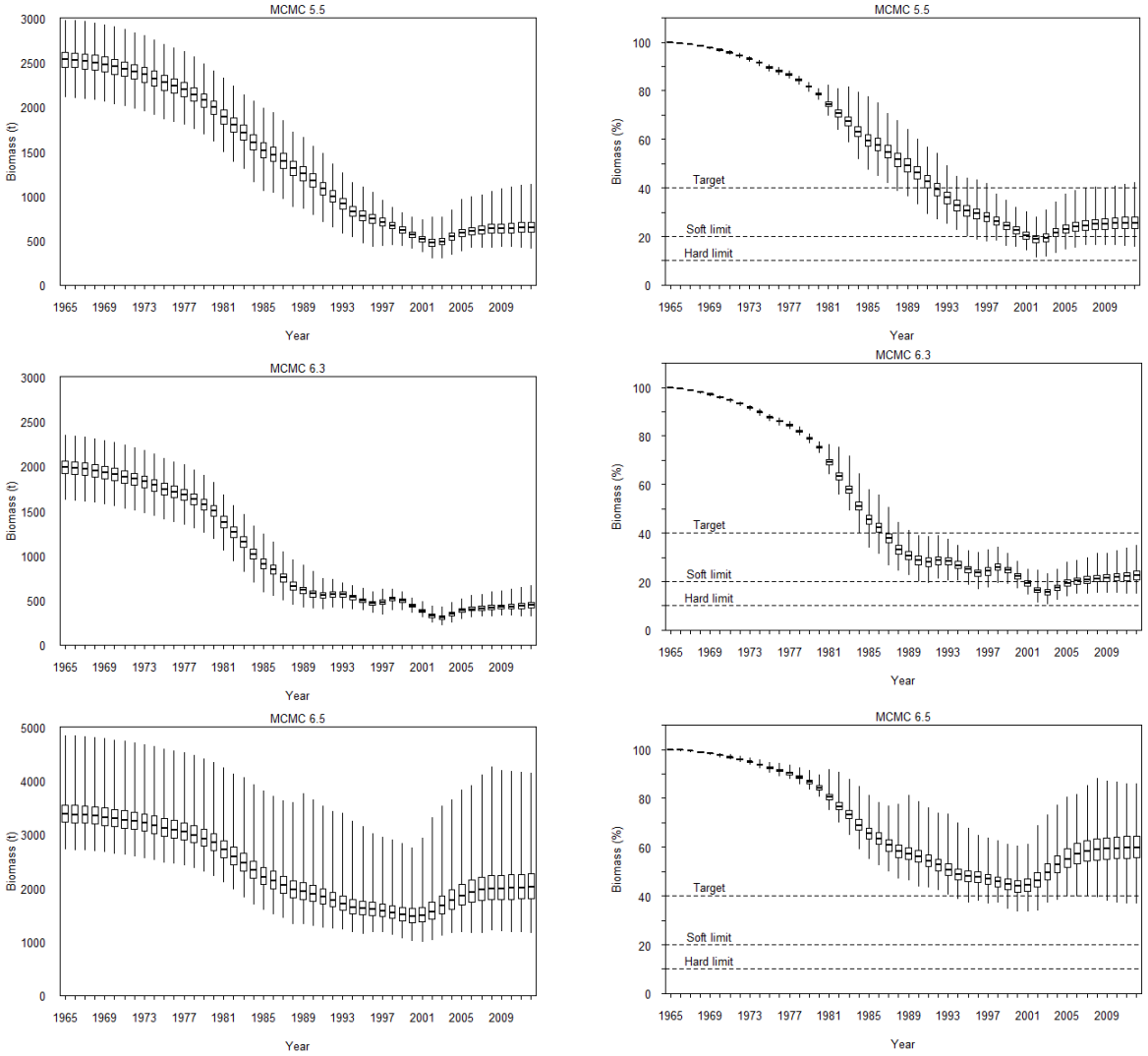

Figure 16: Posterior distributions of spawning stock biomass and spawning stock biomass as a percentage of virgin level from MCMC 5.2, 5.5, 6.3, and 6.5. The box shows the median of the posterior distribution (horizontal bar), the 25th and 75th percentiles (box), with the whiskers representing the full range of the distribution.

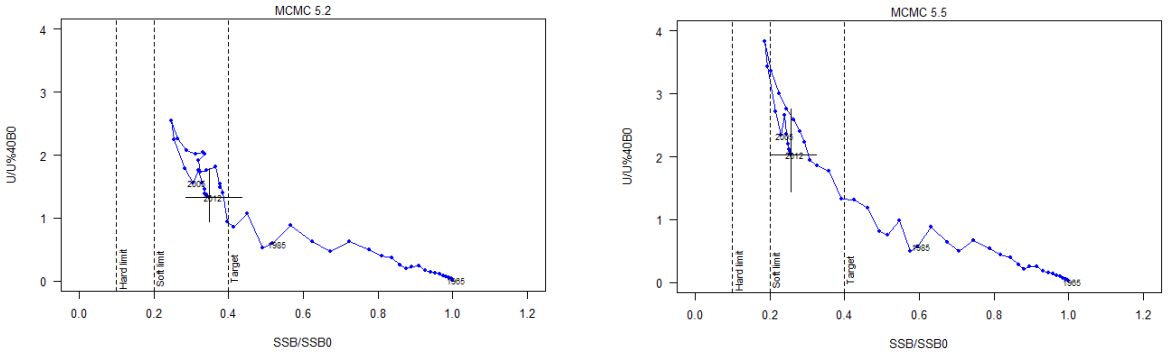

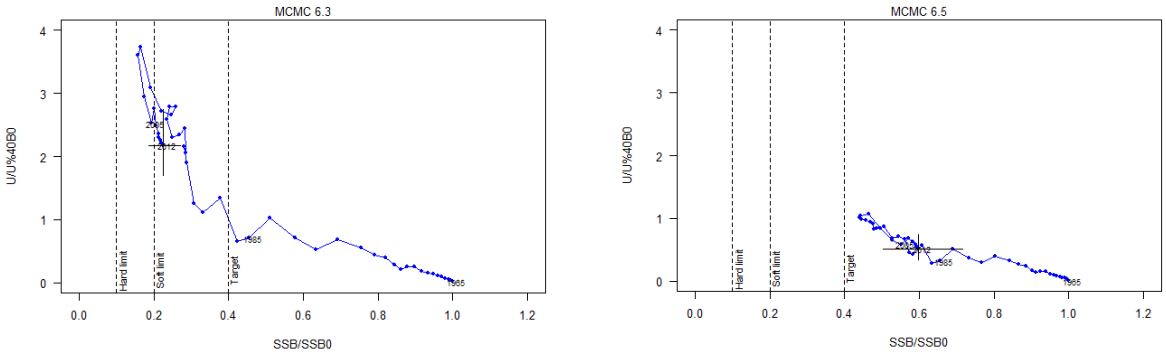

Figure 17: Trajectory of exploitation rate as a ratio $U_{\%40B0}$ and spawning stock biomass as a ratio of B_0 from the start of assessment period 1965 to 2012 for MCMC 5.2 (base case), 5.5 (no early CPUE), 6.3 (fast growth), and 6.5 (slow growth). The vertical lines at 10%, 20% and 40% B_0 represent the soft limit, the hard limit, and the target. Estimates are based on MCMC median and the 2012 90% CI is shown by the cross line.

APPENDIX A: SUMMARY MPD MODEL FITS AND ESTIMATES

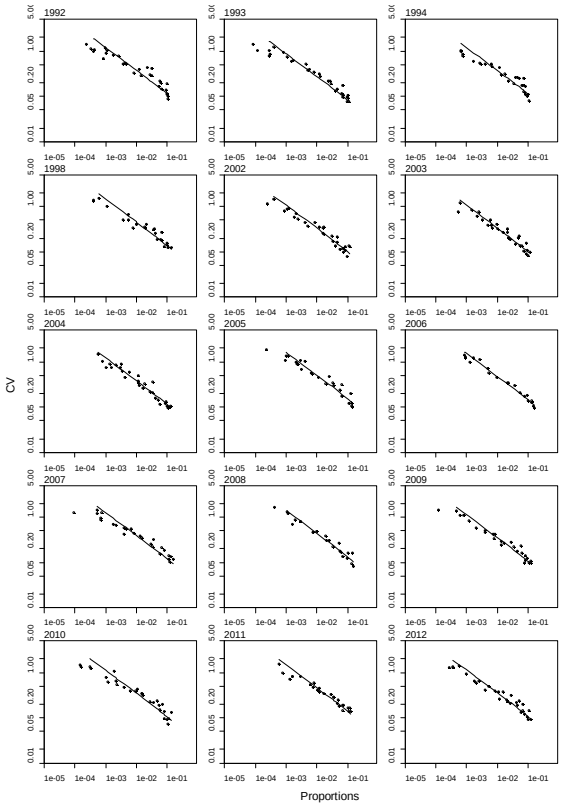

Figure A1: Estimated proportions versus CVs for the commercial catch length frequencies in PAU 5D. Lines indicate the best least squares fit for the effective sample size of the multinomial distribution. Length frequencies 1998, 2002–04, 2007, 2009–2012 were included in the assessment models.

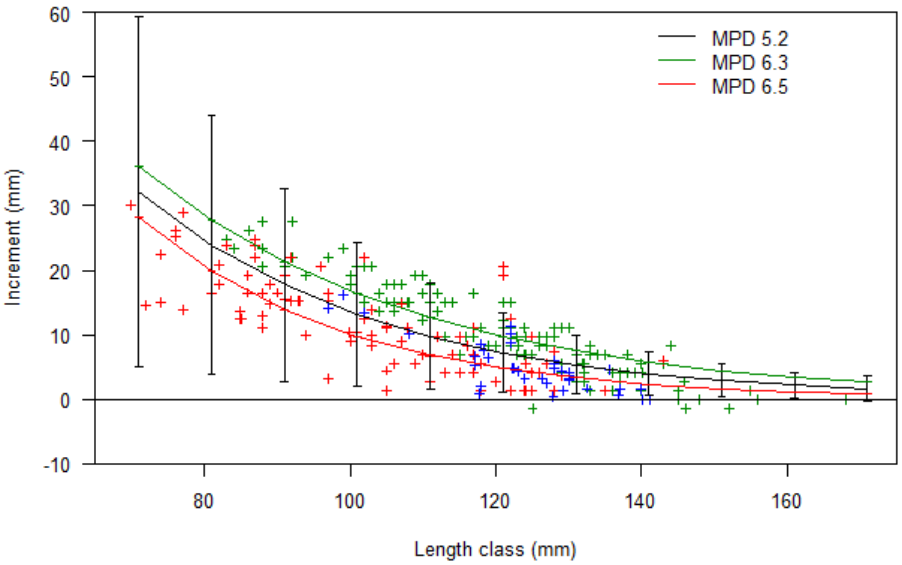

Figure A2: Growth curves used in various model runs. For base case, growth parameters were estimated in the model by fitting to annual growth increments data from Catlin West (green), Catlin East (red), and the east coast (blue). For model 6.3.0, growth parameters were fixed at $g_1 = 32.5$ and $g_2 = 10$; for model 6.5, growth parameters were fixed at $g_1 = 24.5$ and $g_2 = 5$.

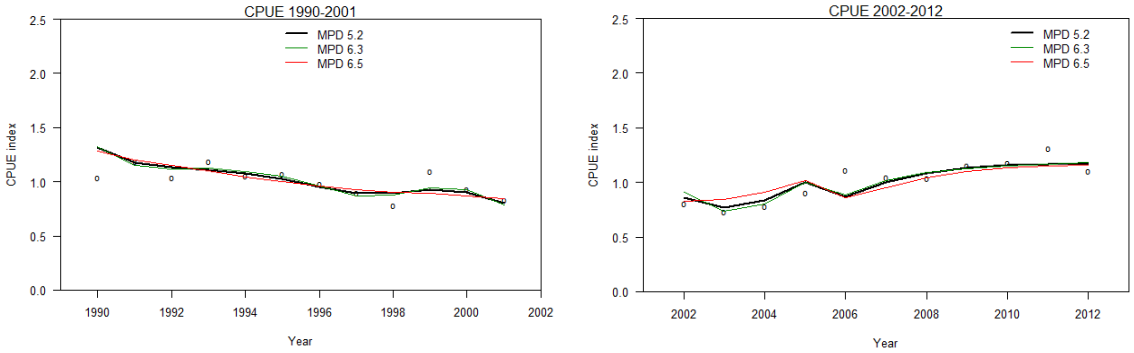

Figure A3: Comparison of fits to the CPUE and PCPUE data for MPD 5.2 (base case) , MPD 6.3 and MPD 6.5.

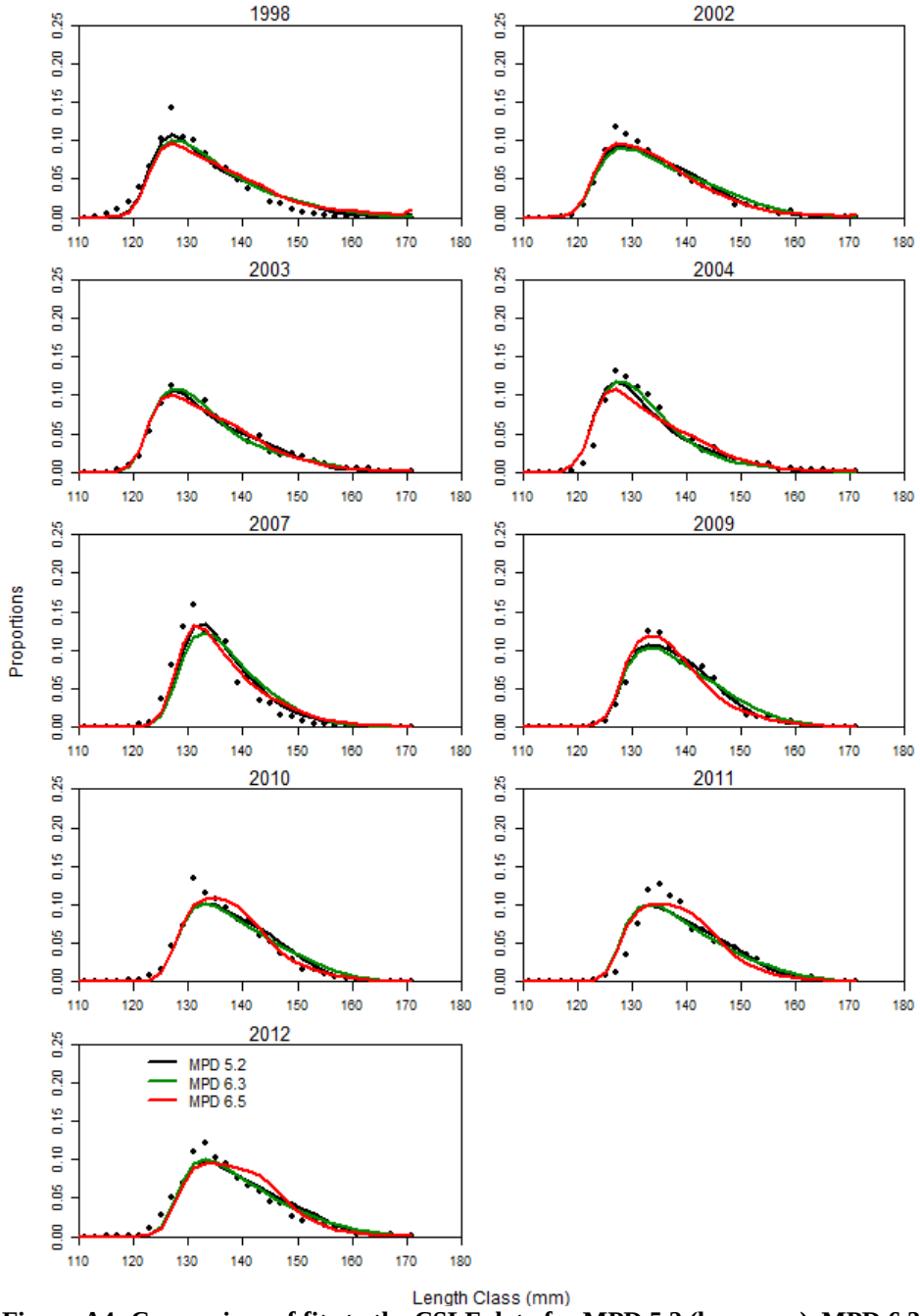

Figure A4: Comparison of fits to the CSLF data for MPD 5.2 (base case), MPD 6.3 and MPD 6.5.

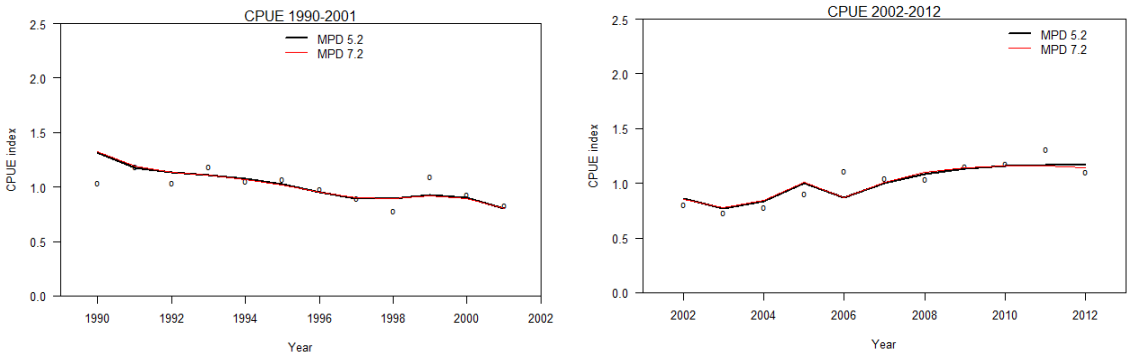

Figure A5: Comparison of fits to the two CPUE datasets for MPD 5.2 (base case) and MPD 7.2.

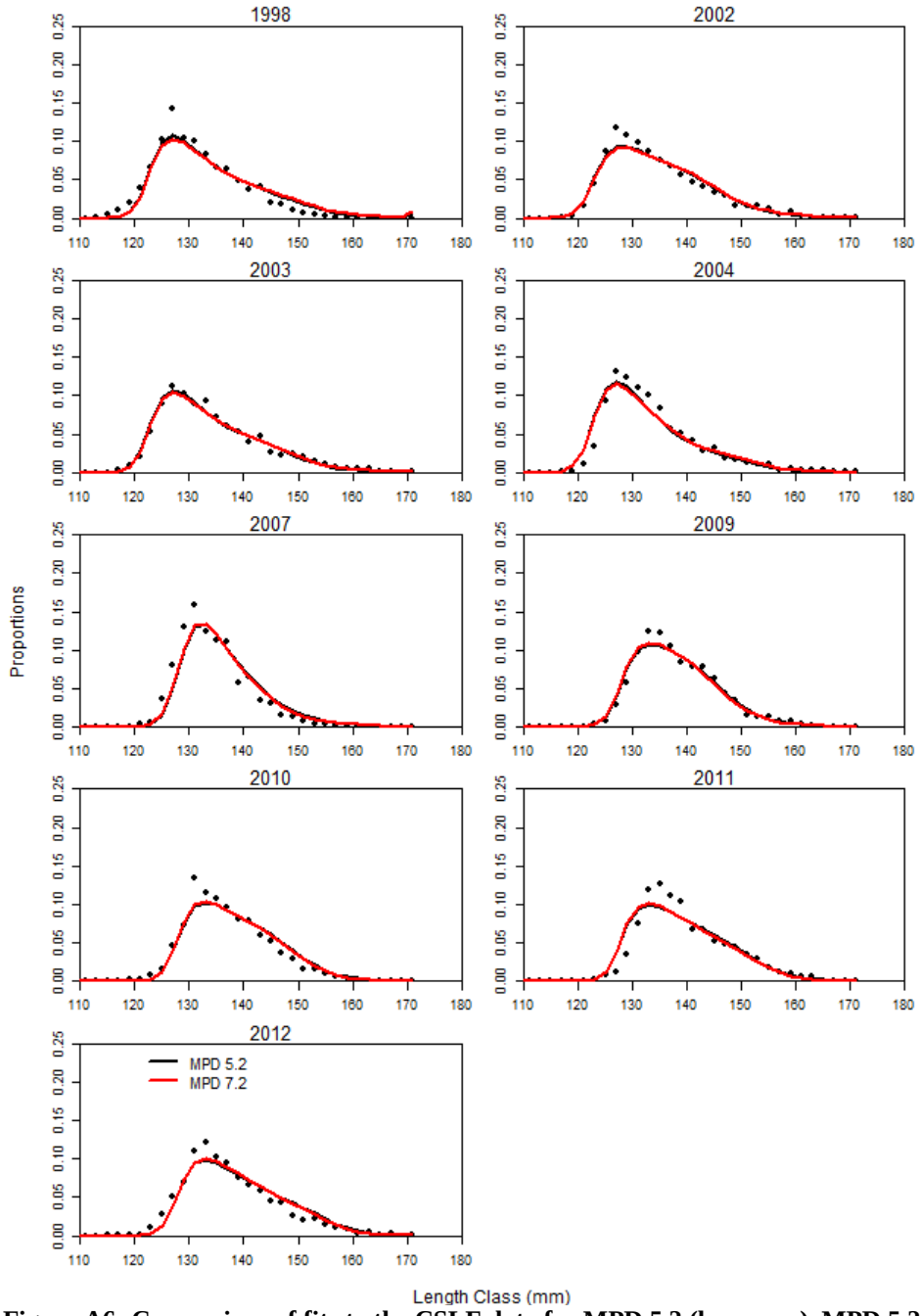

Figure A6: Comparison of fits to the CSLF data for MPD 5.2 (base case), MPD 5.2 and MPD 7.2.

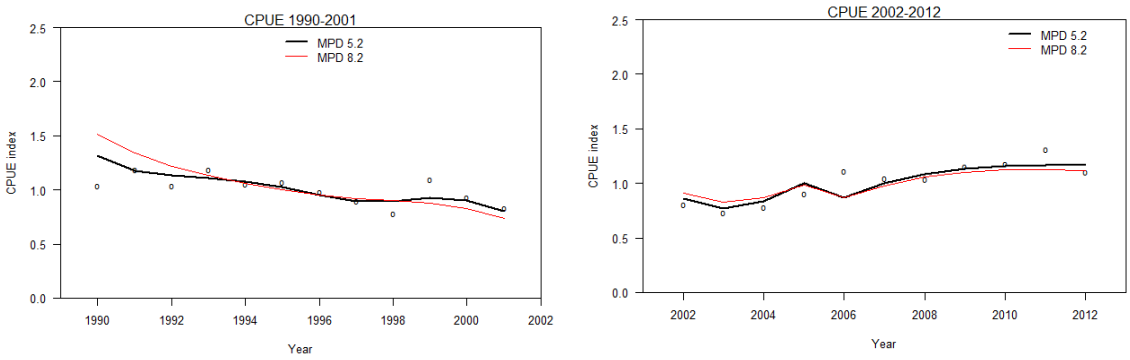

Figure A7: Comparison of fits to the two CPUE datasets for MPD 5.2 (base case) and MPD 8.2.

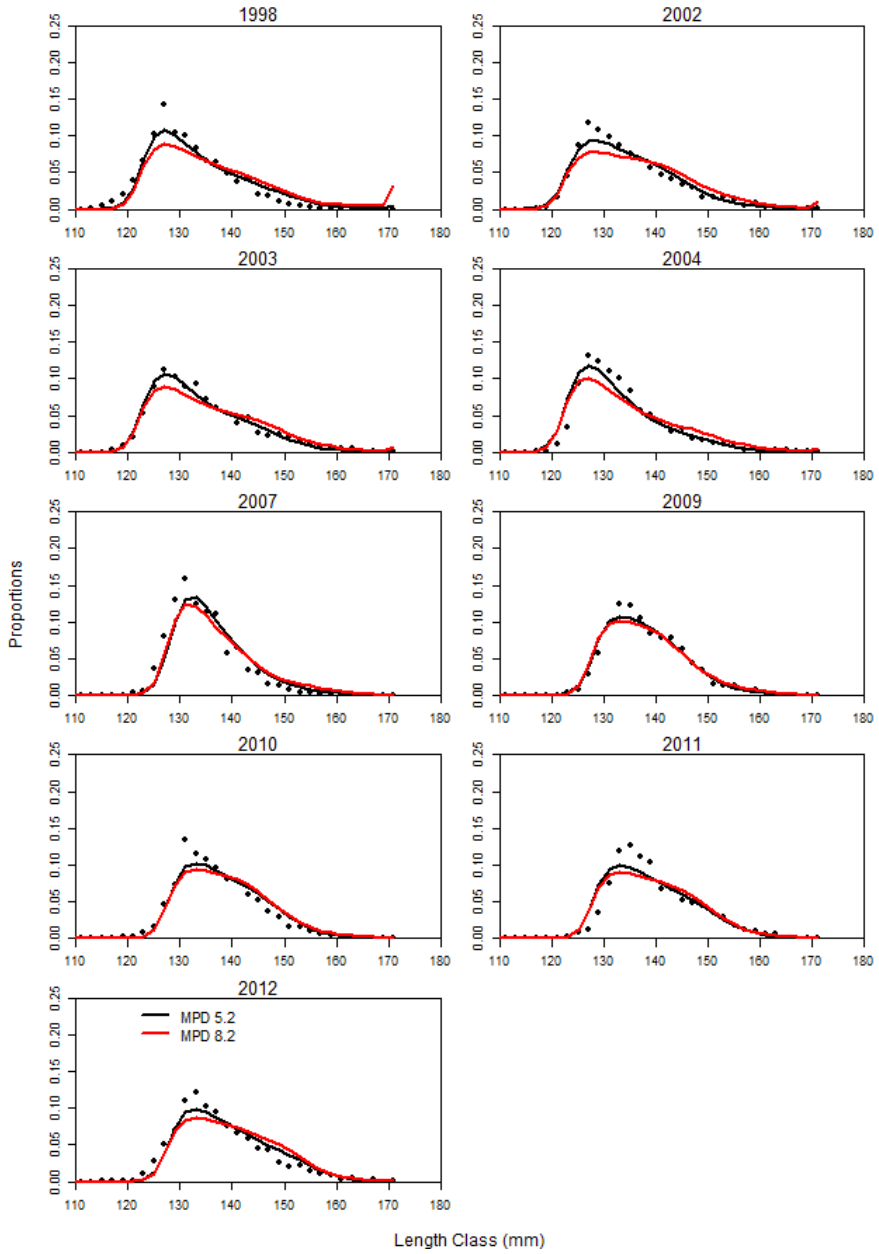

Figure A8: Comparison of fits to the CSLF data for MPD 5.2 (base case), MPD 5.2 and MPD 8.2.

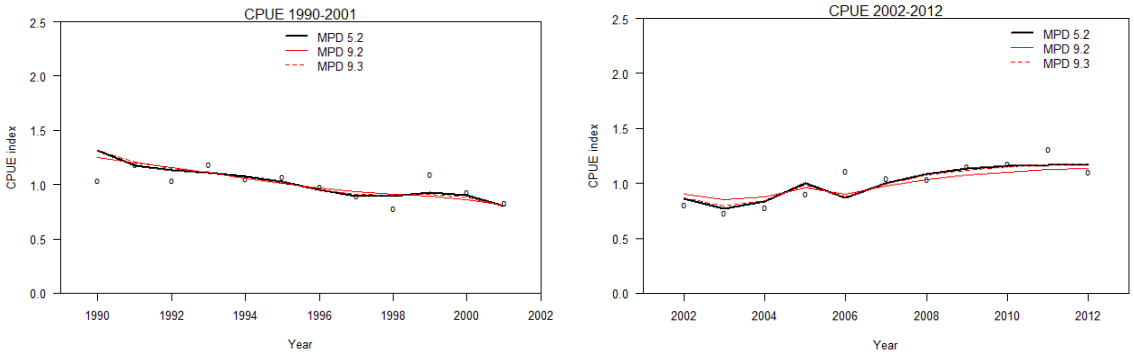

Figure A9: Comparison of fits to the two CPUE datasets for MPD 5.2 (base case), MPD 9.2 and MPD 9.3.